

# Chapter 2

## Sun et Lumière: Solar Wind-Magnetosphere Coupling as Deduced from Ionospheric Flows and Polar Auroras

S.E. Milan

**Abstract** The Dungey (Phys. Rev. Lett. 6:47–48, 1961) open model of the magnetosphere, and especially its time-dependent form, the expanding/contracting polar cap (ECPC) paradigm, has provided an important theoretical framework within which to understand solar wind-magnetosphere-ionosphere coupling. This paper reviews the evidence supporting the open and ECPC models, and discusses developments that have arisen in the last 20 years, concentrating on the contributions made by measurements of the ionospheric convection pattern and global auroral imagery. Various magnetospheric phenomena are discussed within the context of the open model, including substorms, geomagnetic storms, steady magnetospheric convection, sawtooth events, cusp auroral spots, and transpolar arcs. The review concludes with a discussion of avenues for future research in the field of solar wind-magnetosphere-ionosphere coupling.

### 2.1 Introduction

As outlined in Stan Cowley’s preceding paper (chapter “Dungey’s Reconnection Model of the Earth’s Magnetosphere: The First 40 Years”), the pioneering work of Jim Dungey has provided a coherent theoretical framework in which many aspects of the large-scale structure and dynamics of the magnetosphere-ionosphere system can be understood. Development of the open model of the magnetosphere from the original “Dungey cycle” picture (Dungey 1961), to the fully time-dependent “expanding/contracting polar cap” paradigm (ECPC) of solar wind-magnetosphere-ionosphere coupling (Lockwood et al. 1990; Cowley and Lockwood 1992; Lockwood and Cowley 1992) took 30 years. The subsequent 20 years have seen a

---

S.E. Milan (✉)

Department of Physics and Astronomy, University of Leicester, Leicester LE1 7RH, UK

Birkeland Centre for Space Science, Box 7803, 5020 Bergen, Norway

e-mail: [ets@leicester.ac.uk](mailto:ets@leicester.ac.uk)

© Springer International Publishing Switzerland 2015

D. Southwood et al. (eds.), *Magnetospheric Plasma Physics: The Impact of Jim Dungey’s Research*, Astrophysics and Space Science Proceedings 41, DOI 10.1007/978-3-319-18359-6\_2

33

steady accumulation of observational evidence for both Dungey's open model and the ECPC. Alongside this, there has been a growing appreciation that magnetospheric phenomena beyond those originally considered by Dungey and his co-workers fit within the framework provided by the open model. Furthermore, Dungey's ideas have gained increasing application in the study of the magnetospheres of solar system bodies other than the Earth.

The body of literature that provides support for Dungey's picture is too large to be summarized in a brief review. To be focussed, this review confines itself to a discussion of how the availability of global auroral imagery and measurements of the ionospheric convection pattern have helped cement the ideas Dungey put forward at a time when there was a general dearth of observational evidence to support them. What evidence there was came largely from ground-based observations, as described by Cowley (chapter "Dungey's Reconnection Model of the Earth's Magnetosphere: The First 40 Years"), and these helped develop Dungey's ideas. This review is divided into several sections: Sect. 2.2 describes the current understanding of the time-dependent Dungey cycle, the ECPC; Sect. 2.3 describes the observations of the ionospheric convection pattern and auroras which provide evidence for the ECPC; Sect. 2.4 describes how the ECPC and substorm cycle are related; Sect. 2.5 explains how magnetic reconnection rates can be quantified; Sect. 2.6 discusses the current understanding of how magnetotail reconnection is controlled; Sect. 2.7 looks at the role of reconnection in magnetospheric dynamics when the interplanetary magnetic field is directed northwards; and Sect. 2.8 concludes with a brief discussion of future research directions.

## 2.2 The Modern View of the Dungey Cycle: The Expanding/Contracting Polar Cap Paradigm

Dungey proposed that magnetospheric dynamics were driven largely by magnetic reconnection occurring at the magnetopause between the interplanetary magnetic field (IMF) and the terrestrial field. IMF orientation will be discussed in terms of the usual Geocentric Solar Magnetic (GSM) coordinate system, in which the X-axis points towards the Sun, the X-Z plane contains the Earth's magnetic axis, and Y is perpendicular to this, pointing in a generally duskwards direction. In this system, "northwards" and "southwards" directed field relate to IMF  $B_Z > 0$  and  $B_Z < 0$ , respectively. Reconnection was expected to occur most efficiently where the magnetic shear across the magnetopause was high, that is near the subsolar point for southwards-directed IMF (Dungey 1961), and at high latitudes for northward IMF (Dungey 1963). Magnetic reconnection was also proposed to occur between the oppositely-directed magnetic fields either side of the neutral sheet in the magnetotail, especially when the IMF is directed southwards (Dungey 1961). The combined action of subsolar and magnetotail reconnection leads to a circulation of magnetic field and plasma in the magnetosphere in what is now known as the

Dungey cycle (see Fig. 1.2 of chapter “Dungey’s Reconnection Model of the Earth’s Magnetosphere: The First 40 Years”). As remarked by Stan Cowley at the end of his paper, by the mid-1990s it was clear that time dependence of magnetic reconnection at the magnetopause, due to variations in interplanetary conditions, and in the magnetotail lead to a highly dynamic system, in which the proportion of the terrestrial magnetic flux that is open can vary considerably on timescales of minutes and hours. For instance, studies of the location of the dayside magnetopause showed that inward motion occurs as a consequence of erosion by reconnection during southwards IMF, without immediate return of newly-closed flux to the dayside by reconnection in the magnetotail (e.g., Aubry et al. 1970; Haerendel et al. 1978). This decoupling of the dayside and nightside processes leads to a new view of how the Dungey cycle is powered: many workers contributed to the development of this new view, notably Siscoe and Huang (1985) and Freeman and Southwood (1988), culminating in the “expanding/contracting polar cap” paradigm (ECPC), first fully elucidated by Cowley and Lockwood (1992). We describe the ECPC in the rest of this section.

The top row of Fig. 2.1 presents schematics of the magnetic field orientation in the magnetopause of the Earth (white lines), looking from the Sun, and the locations where the magnetic shear is high for different orientations of the IMF (purple lines):  $B_Y > 0, B_Z < 0$ ;  $B_Y > 0, B_Z > 0$ ;  $B_Y = 0, B_Z > 0$ . The magnetopause is roughly paraboloid in shape (with indentations near the cusps) due to stress-balance between the ram pressure of the solar wind and magnetic pressure inside the magnetosphere. In this section, we concentrate on the left column of Fig. 2.1 in which the region of high shear (red) is located across the magnetopause at low latitudes, where terrestrial magnetic flux is closed (green region) rather than open lobe flux (blue region) as found at higher latitudes, tailward of the cusp openings. Once reconnection occurs between the IMF and the terrestrial field, highly-kinked new open field lines evolve across the magnetopause under the influence of the magnetosheath flow (directed radially away from the subsolar point) and the magnetic tension force (Cowley 1981a, b) (see also Fig. 1.9 of chapter “Dungey’s Reconnection Model of the Earth’s Magnetosphere: The First 40 Years”). Figure 2.2 shows the expected motion of the intersection points of newly reconnected field lines with the magnetopause as they join the existing open flux of the lobes (Cowley and Owen 1989; Cooling et al. 2001). For the  $B_Y > 0$  case, tension forces pull northern (southern) hemisphere flux towards the dawn (dusk) sector. The left-middle panel of Fig. 2.1 shows a cross-section of the magnetotail, with the open flux (blue) of the northern and southern lobes, and the closed flux associated with the plasma sheet (green). Across the top of the lobes is indicated the region of newly-opened flux created by reconnection, pulled towards dawn in the northern hemisphere by tension forces, indicating that the tail magnetopause has been deformed from a cylinder; equally, the subsolar magnetopause is eroded by the action of reconnection. Cowley and Lockwood (1992) realized that such deformation of the magnetopause from a paraboloid would result in stress-imbances which lead to motions of the plasma within the magnetosphere to return the system to equilibrium with the solar wind flow (see Fig. 2.3).

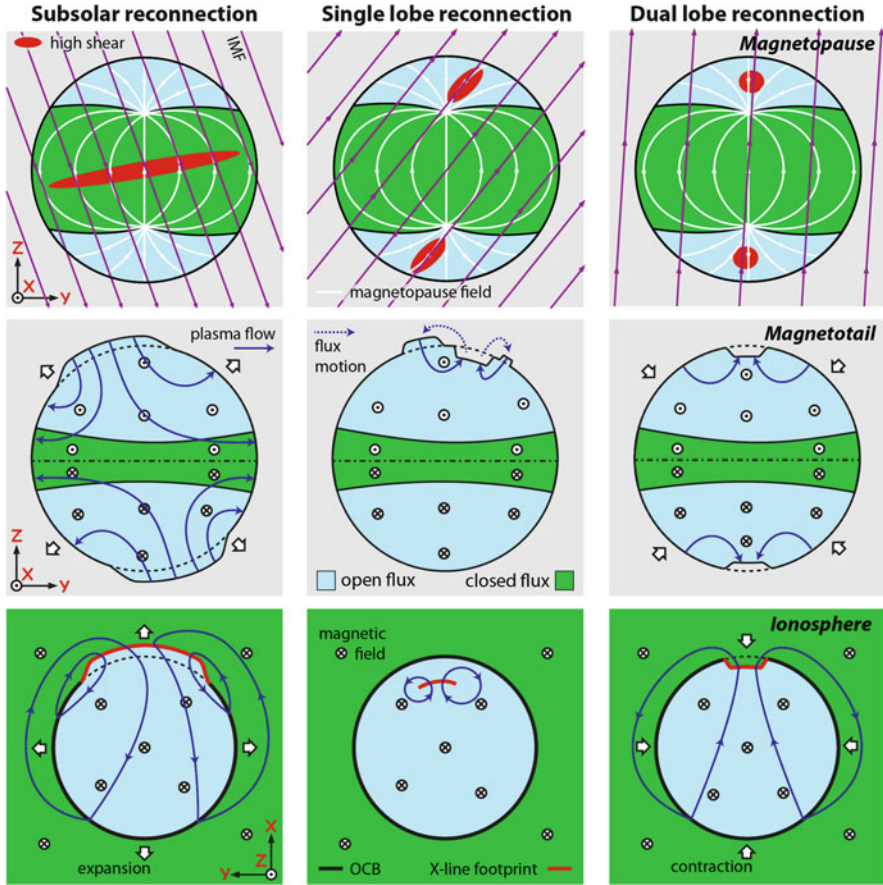


**Fig. 2.1** Schematics of solar wind-magnetosphere-ionosphere coupling. The *upper row* shows the magnetopause looking from the Sun, the *middle row* a cross-section of the magnetotail, the *bottom row* a view of the northern hemisphere ionosphere from above. Green (blue) regions indicate magnetic field lines that are closed (open). Purple arrows indicate the direction of the interplanetary magnetic field, white arrows the direction of the magnetic field in the magnetopause. Dotted and crossed circles indicate the magnetic field direction into or out of the plane of the diagram. Red areas in the upper panels show where the IMF/magnetopause magnetic shear is high and reconnection is likely to occur. In the lower panels, the thick black line indicates the location of the open/closed field line boundary (OCB); the thick red line indicates the ionospheric footprint of the magnetopause reconnection X-line. Blue arrows indicate the direction of plasma motions (and magnetic flux transport) in the magnetotail and in the ionosphere. In the ionosphere, the OCB moves with these plasma flows, but there is relative motion of the flows with respect to the X-line (Color figure online)

The left-bottom panel of Fig. 2.1 shows the magnetic flux of the northern lobe (blue) and plasma sheet (green) mapped into the northern hemisphere. The ionospheric projection of the lobe is known as the polar cap, usually of roughly circular cross-section, centred somewhat antisunwards of the geomagnetic pole; the polar

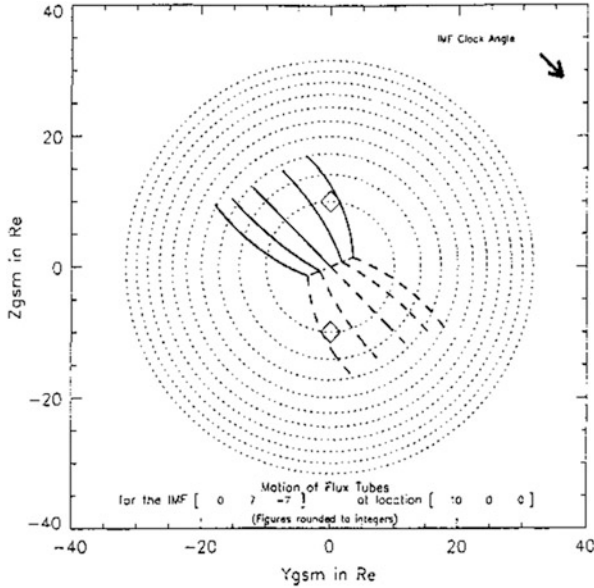


**Fig. 2.2** The motion of the intersection points of five pairs of newly-reconnected field lines away from a subsolar reconnection X-line for IMF  $B_z < 0$ ,  $B_y > 0$ , looking from the Sun. Concentric circles represent the surface of the magnetopause, and diamonds indicate the openings of the cusps [from Cooling et al. (2001)]

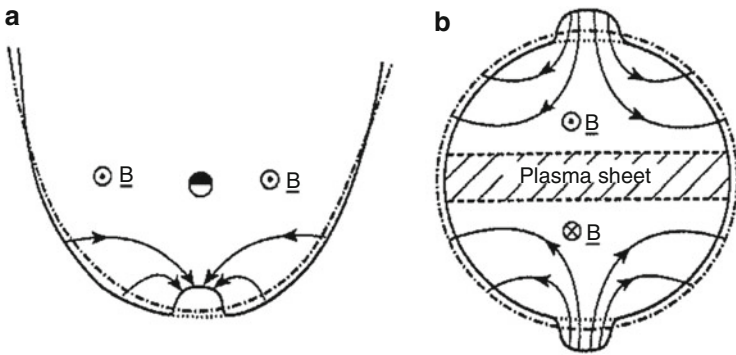


**Fig. 2.3** (a) The magnetopause location in the equatorial plane, showing erosion by a burst of subsolar reconnection and the subsequent plasma flows which return the magnetopause to stress balance with the solar wind flow. (b) Deformation of the magnetotail cross-section by the addition of new open flux to the lobes, and the plasma flows which return it to equilibrium [from Cowley and Lockwood (1992)]

cap boundary (thick black line) is also known as the open/closed field line boundary (OCB). The closed field lines adjacent to the dayside OCB map out through the cusps to the dayside magnetopause whereas on the nightside the OCB maps to the boundary between open and closed field lines in the magnetotail. In this figure, the

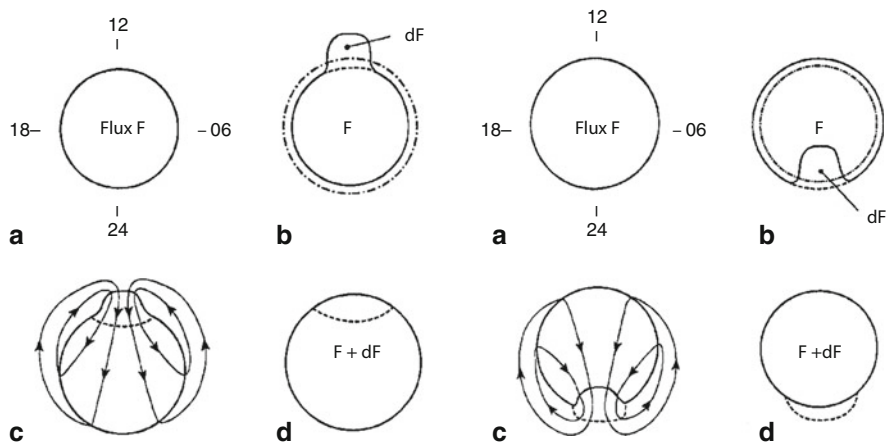


**Fig. 2.4** (*Left*) The addition of new open flux to the polar cap by dayside reconnection, and the flows which are excited by pressure imbalances on the magnetopause. Bursts of dayside reconnection lead to an expansion of the polar cap. (*Right*) The corresponding picture for magnetotail reconnection in which open flux is closed at the nightside OCB and the polar cap contracts [from Cowley and Lockwood (1992)]

region of previously closed flux adjacent to the dayside OCB has been opened by the action of reconnection (the footprint of the active X-line is indicated as a thick red portion of the OCB) and the polar cap is deformed in a similar manner to the tail magnetopause. Cowley and Lockwood (1992) again realized that the flows excited within the magnetosphere by the deformation of the magnetopause (Fig. 2.3) are communicated to the ionosphere and return the polar cap to a circular configuration (left panels of Fig. 2.4). As indicated in the left-bottom panel of Fig. 2.1, within the region of newly opened flux, the magnetic tension forces associated with the  $B_Y > 0$  component of the IMF add a duskwards component to the ionospheric flow; further towards the nightside, a dawnwards component is introduced to the flows due to the asymmetrical addition of new open flux to the northern lobe. Finally, we note that each addition of new open flux to the magnetosphere by dayside reconnection leads to an inflation of the magnetotail lobe and an expansion of the cross-section of the polar cap in the ionosphere, as indicated by white arrows in Fig. 2.1.

This picture provides a unifying framework for understanding the motion of plasma in the magnetosphere and ionosphere as a consequence of low latitude magnetopause reconnection. In this picture, reconnection acts to change the topology of magnetic field lines—an increasing proportion of the flux associated with the Earth’s dipole becoming open—but plasma motions are driven by pressure exerted on the magnetopause by the flow of the solar wind, with a contribution from tension forces on newly opened field lines.

Magnetic reconnection in the magnetotail acts to decrease the proportion of open flux in the magnetosphere: closed field lines are able to return towards the dayside magnetosphere, initially through magnetic tension forces and subsequently through pressure imbalances associated with changes in magnetospheric shape as erosion of

magnetospheric flux on the dayside continues [right panels of Fig. 2.4, from Cowley and Lockwood (1992)]. In this way, each burst of dayside or nightside reconnection leads to a slow shuffling of open flux antisunwards across the polar cap, or equivalently from the high-latitude lobe magnetopause towards the magnetotail neutral sheet.

This picture describes magnetospheric dynamics in terms of changes in the proportion of open flux and the stresses exerted by deviations of the magnetopause from hydrodynamic equilibrium with the solar wind. Stresses are transmitted within the magnetosphere by electric currents: Chapman-Ferraro currents generated at the magnetopause are diverted into the magnetosphere as “region 1” Birkeland currents that flow along magnetic field lines into the ionosphere (field-aligned currents or FACs), Pedersen currents flow across the auroral zone ionosphere, and “region 2” Birkeland currents then connect into the inner magnetosphere where they are subsequently closed through a partial ring current (e.g., Iijima and Potemra 1978; Cowley 2000). These current systems are then a fundamental part of the magnetosphere-ionosphere coupling that delivers stress to the ionosphere to cause it to move in response to changes in magnetospheric structure caused by magnetic reconnection.

The rate of magnetic reconnection at the dayside is dependent on conditions in the interplanetary medium, most importantly the orientation and strength of the IMF, and this will vary on timescales as short as minutes. The rate of magnetic reconnection in the magnetotail cannot instantaneously adjust itself to match the magnetopause rate, resulting in a significant variation in the amount of open flux in the magnetosphere. Changes in the proportion of open flux, and hence the size of the polar cap, are a measure of the global reconnection rates. Quantitatively, the rate of magnetic reconnection—the magnetic flux transferred from a closed topology to an open topology at the magnetopause (or open to closed in the magnetotail) in unit time—has dimensions of  $\text{Wb s}^{-1}$  or equivalently volts (V). The continuity equation for open flux can be expressed as

$$\frac{dF_{PC}}{dt} = \Phi_D - \Phi_N \quad (2.1)$$

where  $\Phi_D$  is the dayside (subsolar magnetopause) reconnection rate and  $\Phi_N$  is the nightside (magnetotail) reconnection rate (e.g., Siscoe and Huang 1985; Lockwood and Cowley 1992; Milan et al. 2007; Lockwood et al. 2009). As discussed in detail by Chisham et al. (2008), the dayside reconnection voltage is equal to the line integral of the motional electric field of the ionospheric plasma convection across the dayside portion of the OCB (indicated in red in the left-bottom panel of Fig. 2.1); similarly, the nightside reconnection rate is equal to the magnetic flux transported across the nightside OCB in unit time. Lockwood (1991) deduced that if it was assumed that the polar cap remains circular as it expands and contracts then the rate of antisunwards transport of magnetic flux across the dawn-dusk meridian—known as the transpolar voltage (TPV) or cross polar cap potential (CPCP), expressed as  $\Phi_{PC}$ —will be given by

$$\Phi_{PC} = \frac{1}{2}(\Phi_D + \Phi_N). \quad (2.2)$$

This transpolar voltage can be determined from observations of the ionospheric convection pattern and is used as a measure of the overall strength of the Dungey cycle, a combination of contributions from both magnetopause and magnetotail reconnection. With suitable assumptions, the global electrostatic potential pattern associated with the ionospheric convection can be solved analytically. Siscoe and Huang (1985) were the first to deduce the relationship between ionospheric convection and an expanding polar cap, driven by dayside reconnection. Increasingly sophisticated models have subsequently been developed, by Freeman and Southwood (1988) to include the effect of non-uniform motion of the OCB, by Freeman (2003) to include the influence of both region 1 and 2 Birkeland FAC systems, and by Milan et al. (2012) and Milan (2013) to include both dayside and nightside reconnection contributions and to model the FAC magnitudes.

This association between dayside and nightside reconnection, magnetic flux transport within the magnetosphere, changes in size of the polar cap, and accompanying ionospheric flows has come to be known as the expanding/contracting polar cap paradigm (ECPC) (e.g., Freeman 2003; Milan et al. 2007). Testing the predictions of the ECPC has been a major endeavour since the 1990s when the ideas were first expressed as a coherent picture by Cowley and Lockwood (1992). In the following sections we discuss the observations that have validated the major predictions of the ECPC.

### 2.3 Observations of Ionospheric Convection and Polar Cap Area

Primary observables for testing the ECPC are the polar ionospheric convection pattern and the location of the polar cap boundary (or OCB) at all local times. There are significant challenges inherent in making observations over the majority of the polar regions at sufficient temporal resolution to capture the time-dependent aspects of the behaviour, one of the major reasons for the relatively slow universal adoption of the ECPC paradigm.

The presence of an ionospheric convection pattern had been inferred by Dungey (1961) from magnetic perturbations associated with the  $S_D$  ionospheric current system, as discussed by Cowley (chapter “Dungey’s Reconnection Model of the Earth’s Magnetosphere: The First 40 Years”). Direct measurement of the electric field driving ionospheric convection, however, was made first in the 1970s by satellites (e.g., Heppner 1977; Heppner and Maynard 1987; Rich and Hairston 1994), and later by radars (e.g., Greenwald et al. 1978; Evans et al. 1980; Foster 1983; Alcayde et al. 1986; Ruohoniemi and Greenwald 1996). Necessarily statistical in nature, these studies were not able to easily investigate time-dependencies in the convection, though they were able to determine the influence of the orientation



Initially, only spatially-limited observations of the time-dependence of convection were available (see for example Fig. 1.11 of chapter “Dungey’s Reconnection Model of the Earth’s Magnetosphere: The First 40 Years”) (e.g., Willis et al. 1986; Etemadi et al. 1988; Lockwood and Freeman 1989). More recently, the Super Dual Auroral Radar Network (SuperDARN) (Greenwald et al. 1995; Chisham et al. 2007) has grown in extent and, under favourable conditions, synoptic maps of the global convection pattern are available. This allows the time-dependence of ionospheric convection flows to be determined, as will be discussed in Sect. 2.4.

Several techniques have been used to determine the location of the open/closed field line boundary, including the poleward edge of the electrojets (e.g., Akasofu and Kamide 1975), the poleward edge of auroral luminosity, determined either from space or from the ground (Meng et al. 1977; Craven and Frank 1987; Frank and Craven 1988; Kamide et al. 1999; Brittnacher et al. 1999; Hubert et al. 2006a), the poleward edge of the region 1 FAC region (e.g. Clausen et al. 2013a, b), the convection reversal boundary (e.g., Taylor et al. 1996), coherent radar backscatter characteristics (e.g., Baker et al. 1995, 1997; Lewis et al. 1998; Lester et al. 2001; Chisham et al. 2008), or a combination of these (e.g., Milan et al. 2003; Boakes et al. 2008). For work when only an approximate size of the polar cap is necessary, this can be characterized from a knowledge of the approximate radius of the auroral oval (Milan 2009; Milan et al. 2009b), the radius of the region 1 Birkeland FAC oval (Clausen et al. 2012), or the lower latitude extent of the ionospheric convection pattern (Imber et al. 2013a).

The left panel of Fig. 2.6 [from Chisham et al. (2008)] shows a typical proton auroral image from the FUV/SI12 instrument onboard the Imager for

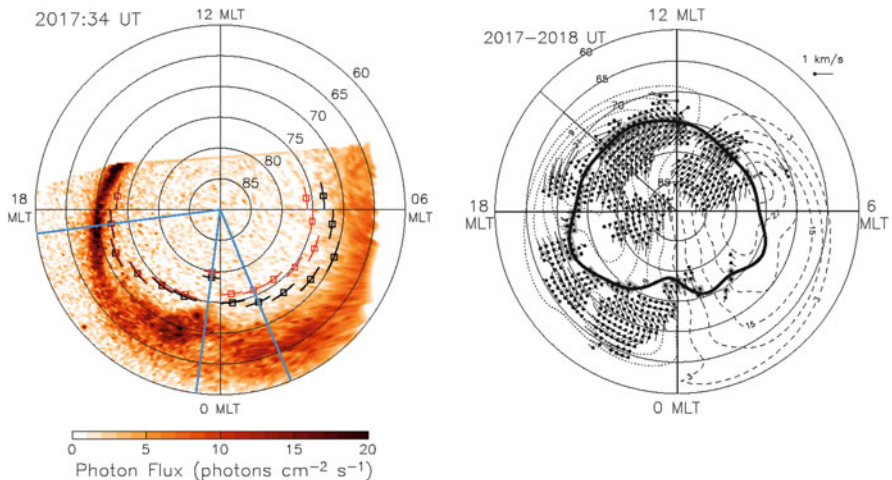


**Fig. 2.6** (Left) An auroral image taken by the SI12 camera onboard the IMAGE spacecraft at 20:17 UT on 26 December 2000. (Right) Simultaneous SuperDARN flow vectors and reconstructed electrostatic potential pattern superimposed over the location of the OCB deduced from the auroral image [from Chisham et al. (2008)]

Magnetopause-to-Aurora Global Exploration (IMAGE) spacecraft (Mende et al. 2000a, b). Red/black lines and squares indicate different estimates of the location of the poleward boundary of emission, using two different techniques, a proxy for the OCB as discussed by Milan et al. (2003). In this particular example, a complete view of the auroral oval is not afforded, and so the full extent of the polar cap cannot be determined. However, when the OCB can be determined (or assumptions made about its location) at all local times, it is possible to use a suitable model of the terrestrial magnetic field,  $\mathbf{B}$ , to determine the magnetic flux threading the polar cap,  $F_{PC}$ , as the surface integral of  $\mathbf{B}$  over the polar cap area:

$$F_{PC} = \int_{PC} \mathbf{B} \cdot d\mathbf{s}. \quad (2.3)$$

Measurements show that  $F_{PC}$  is typically of the order of 0.4 GWb, but can vary between 0.2 and 1 GWb, that is between 2.5 and 12 % of the 8 GWb associated with the terrestrial magnetic dipole (Milan et al. 2007; Coumans et al. 2007; DeJong et al. 2007; Boakes et al. 2009; Huang et al. 2009). The polar caps occupy two roughly circular regions surrounding the magnetic poles with radii close to 1,500 km, but this can vary markedly, especially during geomagnetic storms when expansion of the polar caps drive the auroral zone down to mid-latitudes (Milan 2009), as demonstrated in Fig. 2.7. Long time-scale observations of the size of the polar cap show that there is a considerable solar cycle dependence of the average open flux content of the magnetosphere, with the ionospheric convection pattern, and by inference the polar cap boundary, being expanded to lower latitudes during solar maximum (Imber et al. 2013b).

The full potential of the observations is realized when both the ionospheric flow and the OCB can be imaged. The right panel of Fig. 2.6 shows an interval when both can be characterized. As discussed by Chisham et al. (2008), the dayside and nightside reconnection voltages are the integrals of the motional electric field associated with the ionospheric convection across dayside and nightside portions of the OCB. This is discussed more fully in Sect. 2.5, after first discussing the behaviour of the ECPC during substorm cycles.

## 2.4 The Substorm Cycle and the ECPC

The auroral substorm (Akasofu 1964) is the fundamental mode through which the magnetosphere responds to its interaction with the solar wind. Substorms display two main phases (McPherron 1970; Rostoker et al. 1980; Akasofu et al. 1992): the “growth phase” when the IMF is directed southwards, the polar cap expands, and the auroras move to lower latitudes; the “expansion phase” when nightside auroras

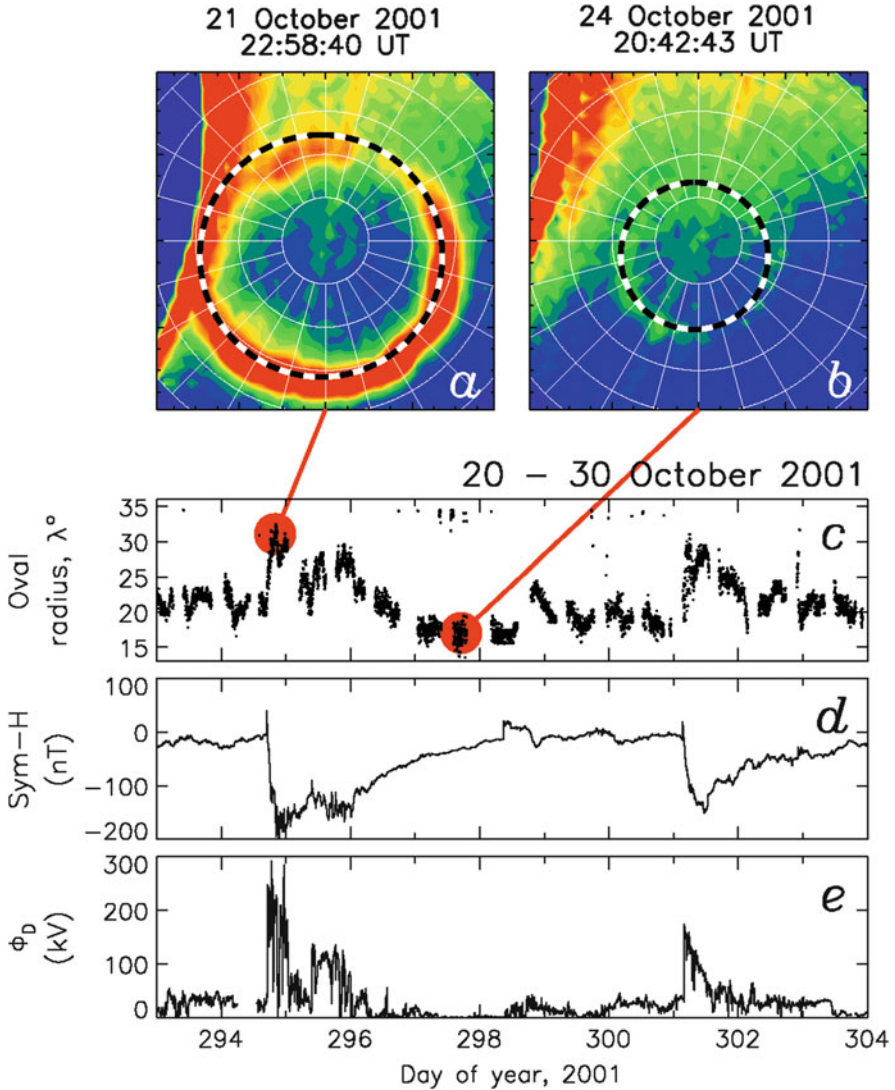


**Fig. 2.7** (a, b) Images of the proton auroral oval from the FUV/SI12 instrument onboard the IMAGE spacecraft. *Dashed circles* indicate circles that have been fitted to the main intensity of the oval. (c) Variations in the radius of the fitted circles, used as a proxy for variations in polar cap size, for the 11-day period 20–30 October 2001. (d) The Sym-H index indicating the occurrence of two geomagnetic storms during this period. (e) A proxy for the dayside reconnection rate, parameterized by upstream interplanetary conditions [from Milan (2009)]

are intensified, the polar cap contracts, and the auroras retreat to higher latitudes. Understanding the substorm in the context of the ECPC is a central plank of validating the paradigm.

Figure 2.8 [from Milan et al. (2007)] shows two examples of the variation of  $F_{PC}$  over several hours (thick grey lines, panel a: 09–16:30 UT on 5 June 1998; panel g: 00–12 UT on 26 August 1998), along with supporting observations. During both intervals,  $F_{PC}$  is seen to vary between approximately 0.2 and 1.0 GWb. When the IMF is directed southwards, that is  $B_Z < 0$  nT (panel d: 09–10, 12–13, 14–16 UT; panel j: 02–05, 10–11 UT) and subsolar reconnection is expected to occur,  $F_{PC}$

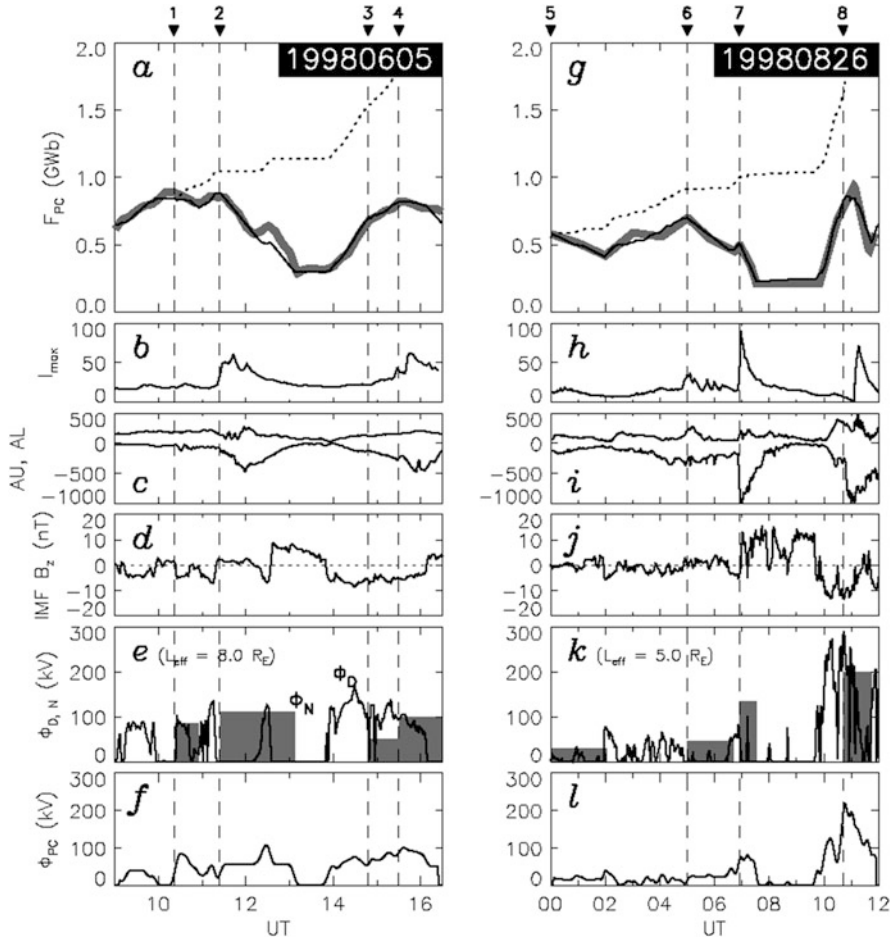


**Fig. 2.8** (a, g) Estimates of the changing polar cap flux,  $F_{PC}$ , for the intervals 09:00–16:30 UT, 5 June 1998, and 00:00–12:00 UT, 26 August 1998 (thick grey lines); superimposed is the time-integral of the dayside and nightside reconnection rates [see Eq. (2.1) and panels e and k]. (b, h) Changes in the maximum auroral brightness in the images (arb. units). (c, i) The AU and AL indices representing the strengths of the ionospheric auroral electrojets. (d, j) The  $B_Z$  component of the IMF as measured by the ACE spacecraft. (e, k) Estimated dayside (black line) and nightside reconnection rates (grey rectangles). The dayside rate,  $\Phi_D$ , is estimated from interplanetary parameters, whereas the nightside rate,  $\Phi_N$ , is fitted to match changes in  $F_{PC}$ . (f, l) The cross-polar cap potential,  $\Phi_{PC}$ , calculated using Eq. (2.2) [from Milan et al. (2007)]

tends to increase, corresponding to an expansion of the polar cap. Significant and rapid contractions of the polar cap, that is decreases in  $F_{PC}$  (panel a: 11:30–13,13:30–16:30 UT; panel g: 05–07, 07–07:30, 11–12 UT), are accompanied by enhancements of the nightside auroral emission intensity seen in the auroral images (panels b and h) and negative excursions of the AL index (panels b and h), both indicative of substorm activity. This indicates that most episodes of rapid reconnection in the magnetotail are associated with the occurrence of substorms, that is substorms play the major role in closing the Dungey cycle, as first suggested in the context of the ECPC by Lockwood and Cowley (1992).

Expansions and contractions of the polar cap should be accompanied by ionospheric flows into the polar cap on the dayside and flows out of the polar cap on the nightside, respectively. Milan et al. (2003) demonstrated that flow into the polar cap during substorm growth phase was indeed consistent with the rate at which it was expanding. The flows out of the polar cap during substorm expansion phase have been harder to identify, though they were observed for a weak isolated substorm by Grocott et al. (2004). Subsequent studies have shown that the nightside flows are considerably complicated by high conductances in the substorm auroral bulge and the frictional coupling between ionosphere and atmosphere that this entails (Morelli et al. 1995; Grocott et al. 2009).

That substorms are associated with open magnetic flux accumulation and closure is corroborated by measurements in the magnetotail which show that the lobe magnetic field strength increases during substorm growth phase, as open flux accumulates in the tail and the magnetopause flares outwards against the ram pressure of the solar wind, only to decrease again after the onset (e.g., Slavin et al. 2002; Milan et al. 2004, 2008). Indeed, measurements of the strength and orientation of lobe magnetic field lines, coupled with a knowledge of the solar wind ram pressure, can be used to infer the open flux content of the magnetosphere (Petrinec and Russell 1996; Shukhtina et al. 2010).

The length of the magnetotail can also be estimated. Dungey (1965) suggested that if lobe field lines remain open for 4 h (approximately the ionospheric convection transit time from the dayside to the nightside of the polar cap), these are stretched to a length of 1,000  $R_E$  by the flow of the solar wind before being disconnected by magnetotail reconnection. Cowley (1991) referred to this as the “connected tail”, and suggested that it is associated with a down-stream wake consisting of highly-kinked, newly-disconnected field lines which would take some time to straighten under the action of the magnetic tension force, the “disconnected tail” which could be five times longer than the connected tail. Milan (2004a) showed that knowledge of the recent history of the size of the polar cap and the dayside and nightside reconnection rates allows the length and flux content of the magnetotail lobes to be quantified, and showed that, somewhat counter-intuitively, the magnetotail is longer during quiet magnetospheric periods than disturbed periods. During northwards IMF conditions dayside and nightside reconnection rates are low and any pre-existing open flux lengthens at the solar wind flow speed. When dayside reconnection recommences, following a southward

turning of the IMF, nightside reconnection will eventually be triggered, and the oldest, longest open field lines will be removed from the system.

## 2.5 Quantifying Reconnection Rates

As dayside and nightside reconnection are key to understanding the dynamics of the magnetosphere, we wish to quantify the rates at which these processes occur, either through (in)direct measurement or through the use of empirically-determined relations (“proxies”) between, say, interplanetary conditions and the magnetopause reconnection rate. As the variation in  $F_{PC}$  is a competition between the creation of open flux at the magnetopause and the subsequent closure of flux in the magnetotail [Eq. (2.1)], observations of  $F_{PC}$  can be used to assess reconnection rates. However, observations of  $dF_{PC}/dt$  alone are not sufficient to determine both  $\Phi_D$  and  $\Phi_N$  independently, only the difference between them. Two different approaches are available to quantify either  $\Phi_D$  or  $\Phi_N$ , or both. In the first,  $\Phi_D$  or  $\Phi_N$  can be determined if assumptions are made regarding the value of the other, for instance

$$\Phi_N \approx \Phi_D^* - \frac{dF_{PC}}{dt} \quad (2.4)$$

where  $\Phi_D^*$  is a proxy for  $\Phi_D$ . It has long been known that the dayside reconnection rate is controlled by the interplanetary conditions upstream of the Earth. One of the first and simplest proxies used is the “half wave rectified solar wind electric field”,

$$\Phi_D^* \propto V_X B_S, \quad (2.5)$$

where  $V_X$  is the solar wind flow speed and  $B_S$  is the southward component of the IMF, that is  $B_S = |B_Z|$  if  $B_Z < 0$  nT and  $B_S = 0$  otherwise (Burton et al. 1975; Holzer and Slavin 1978, 1979). This relates the reconnection rate to the interplanetary magnetic flux transported towards the Earth per unit length along the GSM Y-axis. The constant of proportionality in Eq. (2.5) should be related to the width of the channel in the solar wind that impinges on the magnetopause and reconnects, which was estimated to be between 10 and 20 % of the width of the magnetosphere (Reiff et al. 1981).

Milan (2004b) and Milan et al. (2007) used Eq. (2.5) with an “effective length”  $L_{eff}$  between 5 and 8  $R_E$  (Earth radii) to estimate  $\Phi_D^*$  (Fig. 2.8e, k, black line labelled  $\Phi_D$ ) and hence the expected accumulation of open flux, the increase in  $F_{PC}$ , in the absence of nightside reconnection (Fig. 2.8a, g, dashed lines). Discrepancies between the observed  $F_{PC}$  and the modelled allows periods of nightside reconnection to be identified, and a rough estimate of the rate and duration of reconnection (Fig. 2.8e, k, grey rectangles). The episodes of nightside reconnection so identified match periods of substorm activity as described above, as well as smaller events when auroral brightness or geomagnetic indices indicate magnetotail

activity. In a survey of 25 flux closure events, Milan et al. (2007) estimated that on average 0.25 GWb of flux were closed over a duration of 70 min at a reconnection rate near 90 kV; similarly, DeJong et al. (2007) found a 30 % decrease in polar cap area during substorms.

A similar argument was used by Milan et al. (2012) to determine the optimum functional form for  $\Phi_D^*$ . Substorm growth phases were studied, during which it was assumed that  $\Phi_N = 0$ . Various interplanetary parameters including solar wind speed, density, IMF magnitude and orientation were fitted to the observed expansion of the polar cap, yielding the proxy

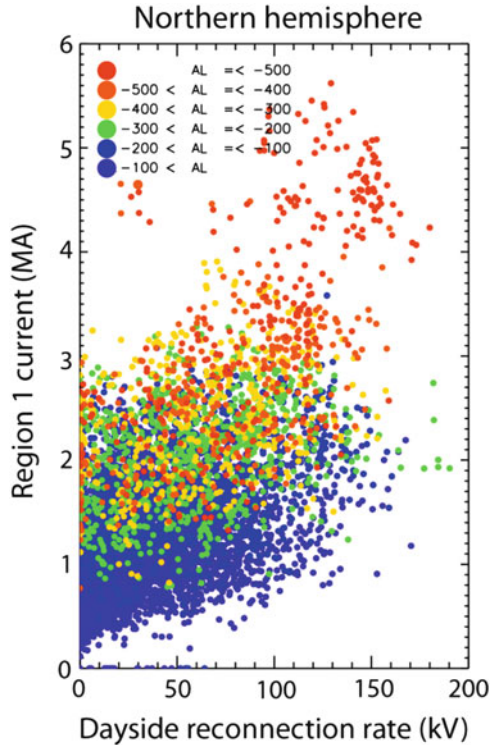
$$\Phi_D^* = 3.3 \times 10^5 V_X^{4/3} (B_Y^2 + B_Z^2)^{1/2} \sin^{9/2} \theta \quad (2.6)$$

where  $\theta$  is the IMF clock angle. Interestingly, it was found that solar wind density did not play a role in the parameterization.

Both  $\Phi_D$  and  $\Phi_N$  can be measured with observations of the ionospheric plasma flow across the OCB, as described in detail by Chisham et al. (2008). Local estimates of the reconnection electric field can be found along limited portions of the OCB, or the overall dayside and nightside reconnection voltages can be determined if observations are available at all local times around the OCB. Unfortunately, the requirement of global auroral images (or another method of OCB location) and excellent determination of the global ionospheric convection pattern means that this technique is only applicable in a limited number of cases. Local estimates of the dayside reconnection electric field were provided by Baker et al. (1997) and Blanchard et al. (2001); an estimate of the voltage along the whole dayside portion of the OCB by Milan et al. (2003) demonstrated that the dayside reconnection voltage was consistent with the observed expansion rate of the polar cap during a substorm growth phase (assuming  $\Phi_N = 0$ ). Local nightside reconnection rates were investigated by de la Beaujardiere et al. (1991) confirming that flow out of the polar cap across nightside OCB was elevated during substorm expansion phase. Full determination of both dayside and nightside reconnection rates using combined global auroral imaging and SuperDARN radar flows, similar to the right panel of Fig. 2.6, by Hubert et al. (2006a), allowed them to show that substorm expansion phase could be associated with nightside reconnection rates as high as 120 kV and that pseudo-breakups occurring during substorm growth phase were associated with modest tail reconnection as well.

An alternative means of determining the contributions of dayside and nightside reconnection to changes in the size of the polar cap and ionospheric convection is to measure the spatial- and time-dependence of the Birkeland current system using the Active Magnetosphere and Planetary Electrodynamics Response Experiment or AMPERE (Anderson et al. 2000, 2002; Clausen et al. 2012). Clausen et al. (2012, 2013a, b) have demonstrated that the region 1 and 2 current ‘‘ovals’’ expand and contract in response to substorms and storms in a manner consistent with the ECPC. Moreover, the strengths of the currents, which are related to the strength of the ionospheric convection, are seen to respond to both dayside and nightside

**Fig. 2.9** The magnitude of the current flowing in the region 1 Birkeland current system in the northern hemisphere during the month of February 2010, as determined from the AMPERE experiment. The position of each *dot* represents the magnitude of the current as a function of a proxy for the dayside reconnection rate; the *colour* represents magnitude of the AL index, which is used as a proxy for the nightside reconnection rate (figure courtesy of J. C. Coxon) (Color figure online)



contributions (J. C. Coxon, private communication). Figure 2.9 presents measurements of the region 1 current strength in the northern hemisphere from each 10 min interval during February 2010, plotted as a function of a dayside reconnection proxy [Eq. (2.6)], and colour-coded with the concurrent AL index, more negative values of which indicate substorm activity and hence nightside reconnection. The currents increase with  $\Phi_D^*$ , but there is a large spread in values of current for a particular reconnection rate, with higher currents at increasingly negative AL. These data suggest, then, that convection is greater when both dayside and nightside reconnection contribute, consistent with Eq. (2.2) and models of the relation between currents and reconnection (e.g., Milan 2013).

## 2.6 What Triggers and Controls Nightside Reconnection?

Studies to date, including those described above, suggest that the dayside subsolar magnetic reconnection rate is closely determined by conditions in the interplanetary medium, though there is some debate as to why this should be (e.g., Borovsky et al. 2008) and there is still not a good characterization of transpolar voltage saturation during extreme solar wind conditions and a variety of possible

explanations (e.g., Siscoe et al. 2002, 2004; Shepherd 2006). Once open flux accumulates through dayside reconnection the magnetosphere must close it again through reconnection in the magnetotail. Although the Dungey cycle and expanding/contracting polar cap paradigms make this clear, and allow a quantitative treatment of magnetic flux transport within the magnetosphere and the attendant ionospheric convection, they do not provide a means of determining when and at what rate the magnetosphere will do this. Much work has been undertaken to understand magnetic flux release in the magnetotail, including the related questions of why it occurs largely in an episodic manner and what triggers it when it does occur.

As described above, substorms play a major role in flux closure. It is thought that the magnetotail reconnection that achieves this occurs in two phases. There is some debate regarding whether a low level of reconnection between lobe field lines is continuously on-going at a distant neutral line or X-line (DXL), perhaps many 10 s of  $R_E$  down-tail. The apparent lack of flux closure during non-substorm times (see Fig. 2.8) puts a rather stringent limit on the rate at which this occurs. Substorms are associated with the formation of a near-Earth X-line (NEXL) in the vicinity of 20  $R_E$  down-tail (e.g., Baker et al. 1996). Initially, reconnection must occur between the closed field lines of the plasma sheet, at what is expected to be a low rate due to the mass-loading of the reconnection site and the corresponding low Alfvén speed. Once reconnection proceeds onto the open field lines of the lobes, which are largely devoid of plasma, the rate can increase. It is at this stage that open flux is closed and changes in polar cap size should begin to be evident. As the substorm proceeds, the NEXL may migrate down the tail to occupy the posited location of the DXL.

The flux closure during a substorm is accompanied by charged particle precipitation producing auroral brightenings, enhancements of the ionospheric conductivity, ionospheric convection enhancements, and auroral electrojet activations. The magnitude of these signatures can be used as an indicator of the “energy” of the substorm. It is well known that substorms come in many sizes and that the location of the initial auroral brightening associated with the substorm can occur over a wide range of latitudes (e.g., Frey et al. 2004). The onset latitude can be considered a proxy for the expansion of the auroral oval, the size of the polar cap, and hence the open flux content of the magnetosphere at the time of onset. It has been demonstrated that substorm energy is closely correlated to the open flux content of the magnetosphere prior to onset (e.g., Akasofu and Kamide 1975; Kamide et al. 1999; Milan et al. 2009a). The amount of flux closed during substorms is also related to the open flux content prior to onset (Shukhtina et al. 2005; Milan et al. 2009a).

Energetic substorms which close a lot of flux might be expected to occur when the dayside accumulation of open flux is rapid, though it is not clear if enhanced flux closure should be effected by a few large substorms or many smaller substorms. A study of the occurrence rate of substorms and the flux closed in each substorm suggested that both increased in approximate proportion to  $\Phi_D^{1/2}$  such that the nightside flux closure rate matched the open flux production rate at the dayside (Milan et al. 2008). It can also be shown that the probability that a substorm will initiate in the near future increases as the open flux content increases (Milan

et al. 2007; Boakes et al. 2009). However, these observations do not explain why “weak” substorms occur on a contracted oval while on other occasions the magnetosphere allows itself to accumulate a large quantity of open flux before initiating an energetic substorm.

It is natural to think that as the magnetosphere accumulates open flux, and the magnetic and plasma pressure in the magnetotail increase, conditions in the vicinity of the neutral sheet become more favourable for the onset of reconnection and that at some point reconnection acts as a “pressure release valve”. However, the studies described above clearly indicate that there is no fixed open flux “threshold” at which substorms are triggered (Boakes et al. 2009); equally, studies of magnetic pressure build-up in the magnetotail prior to onset show that a fixed pressure threshold does not exist either (e.g., Milan et al. 2008).

The level of open flux at which substorms occur has been shown to increase during geomagnetic storms (Milan et al. 2008, 2009b), the signature of which is an enhanced ring current and the magnetic perturbation produced by this as measured by negative excursions of the  $D_{st}$  and Sym-H indices (see Fig. 2.7). It has been speculated that geomagnetic storms produce conditions in the magnetotail which disfavour the onset of reconnection and hence lead to greater accumulation of open flux before it is released. For instance, Kistler et al. (2006) have shown that the concentration of heavy ions in the plasma sheet increases during storms, and it has been suggested that the associated decrease in Alfvén velocity impedes fast reconnection (e.g., Ouellette et al. 2013). Alternatively, Milan et al. (2008, 2009b) have suggested that the magnetic perturbation associated with the enhanced ring current dipolarizes the magnetotail, halting the onset of reconnection until the lobe pressure builds up to produce a sufficiently “tail-like” field once again.

The substorm cycle is not the only “mode” by which the magnetosphere releases open magnetic flux accumulated at the dayside. Other modes that have been described include sawtooth events and steady magnetospheric convection (SMC) events. Sawtooth events display a large and very regular  $\sim 3$  h expansion and contraction cycle of the polar cap (DeJong et al. 2007; Hubert et al. 2008; Huang et al. 2009), and are named after the characteristic appearance of geosynchronous orbit trapped particle fluxes—a gradual drop out of fluxes during the growth phase and a sudden increase at onset (Belian et al. 1995). At present, it is not clear if these are a fundamentally different mode of coupling, or whether they are an extreme example of the substorm cycle occurring during strong solar wind driving conditions in the main phase of geomagnetic storms (Cai et al. 2011). SMCs, on the other hand, do not show an expansion/contraction cycle, the polar cap remaining of approximately uniform size (DeJong and Clauer 2005; DeJong et al. 2008), even though dayside driving and magnetospheric and ionospheric convection are on-going (e.g., McWilliams et al. 2008). In this case, Eq. (2.1) indicates that the nightside reconnection must closely match the dayside rate—hence lending them the alternative name “balanced reconnection intervals” (BRIs) (DeJong et al. 2008)—and by Eq. (2.2) the transpolar voltage must be equal to both. Many SMCs appear to start with a substorm (Sergeev 1977; Kissinger et al. 2012a). Milan et al. (2006) investigated a substorm that displayed repeated dipolarizations during

a  $\sim 2$  h expansion phase which only subsided once the IMF turned northwards and dayside reconnection abated: this suggests that SMCs may be prolonged substorms that maintain reconnection in the tail because dayside reconnection continues after onset, a “driven recovery phase” as described by DeJong et al. (2008). How the magnetosphere achieves this, and if the nightside rate adjusts itself if the dayside rate changes are unclear. Kissinger et al. (2012b) have demonstrated that magnetospheric convection avoids the inner magnetosphere during SMCs and Juusola et al. (2013) suggest that the magnetic perturbation associated with an enhanced ring current leads to reconnection occurring further down-tail than during substorms.

Some workers have suggested that substorms, SMCs, and sawtooth events represent a spectrum of responses of the magnetosphere to different conditions in the interplanetary medium and differing levels of solar wind-magnetosphere coupling (Cai et al. 2006; Partamies et al. 2009). On the other hand, it is possible that preconditioning of the magnetosphere is necessary to drive it into one particular mode of response (e.g., Kissinger et al. 2012b; Juusola et al. 2013). Alternatively, the work of Grocott et al. (2009) suggests that enhanced ionospheric conductivity in the substorm auroral bulge during very disturbed conditions leads to frictional coupling between the ionosphere and atmosphere (“line-tying”) that can inhibit steady ionospheric flows and, as a consequence, steady magnetospheric convection.

As discussed earlier, the accumulation of open magnetic flux in the magnetotail lobes increases the internal pressure of the tail as it inflates against the flow of the solar wind on the outside (Coroniti and Kennel 1972; Petrinec and Russell 1996), which is thought to play a role in the initiation of nightside reconnection. A sudden increase in solar wind ram pressure also acts to increase the internal tail pressure, and there are many documented cases of this triggering reconnection and substorm onset (Boudouridis et al. 2003; Milan et al. 2004; Hubert et al. 2006b, 2009). Northward turnings of the IMF have also been implicated in the triggering of substorms (e.g., Caan et al. 1978; Lyons et al. 1997; Hsu and McPherron 2002), but several refutations also exist (Morley and Freeman 2007; Wild et al. 2009) and many cases where substorms occur without apparent external triggers (e.g., Huang 2002).

## 2.7 Reconnection During Northward IMF

The most active magnetospheric conditions tend to occur during periods of prolonged southward IMF, but many interesting phenomena occur when the IMF is directed northwards as well. Dungey (1963) proposed that reconnection would occur between northward IMF and terrestrial field lines tailwards of the cusps. Cowley (1981b) proposed several scenarios (see Fig. 1.10 of chapter “Dungey’s Reconnection Model of the Earth’s Magnetosphere: The First 40 Years”) in which reconnection took place with closed or open magnetospheric field lines and independently or with the same interplanetary magnetic field line in the two

hemispheres. These different scenarios lead to different predictions regarding the dynamics driven in the magnetosphere.

In an open magnetosphere, it is likely that northwards IMF reconnection will take place with open lobe field lines, termed “lobe reconnection”. If the IMF has a significant  $B_Y$  component, different interplanetary field lines will reconnect at northern and southern reconnection sites (see Fig. 2.1, middle column). This is known as “single lobe reconnection” or SLR, even though it may be happening in both hemispheres simultaneously, though possibly at different rates. In the event that there is only a small  $B_Y$  component the same interplanetary field line might reconnect in both hemispheres, “dual lobe reconnection” or DLR (Fig. 2.1, right column). In the case of SLR, flux is neither opened nor closed and the polar cap size remains of constant size. However, the combination of tension forces on newly-reconnected field lines and deformations of the magnetopause by the redistributed open flux result in “lobe stirring” in the ionosphere, sunward flow at the footprint of the reconnection line and the formation of “reverse lobe convection cells” (Cowley and Lockwood 1992; Huang et al. 2000; Milan et al. 2005b); such reverse cells are just discernible in the average convection pattern for northward IMF in Fig. 2.5. Magnetosheath plasma injected on the newly reconnected, sunward moving field lines displays a “reverse ion dispersion” (Woch and Lundin 1992), and auroras associated with this precipitation can form a “cusp auroral spot” (Fig. 2.10a) (Milan et al. 2000; Frey et al. 2002). Changes in the  $B_Y$  component of the IMF change the location on the magnetopause at which the antiparallel condition is met, and the local time of the cusp spot, indicating the mapping from the magnetopause, moves accordingly (Fig. 2.10b). In the central panel of Fig. 2.1, the effect of reconnection is shown only in the northern lobe, to emphasize that the rate of reconnection in each hemisphere is independent of the other, and may even be absent in one.

As IMF  $B_Y$  becomes small, DLR becomes possible, closing open flux (Fig. 2.1, right column). Imber et al. (2006) suggested that a signature of DLR should be ionospheric convection out of the polar cap across the dayside OCB and a corresponding contraction of the polar cap as open flux is closed. Examples of this signature have been reported (Imber et al. 2006, 2007; Marcucci et al. 2008). The observed length of the footprint of the X-line in the ionosphere allowed Imber et al. (2006) to estimate that DLR should only occur for IMF clock angles less than  $10^\circ$ ; they were also able to demonstrate that DLR had the potential to be an extremely efficient method of solar wind capture by the magnetosphere, and could easily supply the plasma seen to accumulate in the “cold dense plasma sheet” during prolonged periods of northwards IMF (e.g., Øieroset et al. 2005).

Episodic nighttime closure of flux occurs during northward IMF, but at a much reduced rate. These events were first identified as bursts of rapid azimuthal ionospheric convection in the midnight sector close to the boundary of the polar cap (Senior et al. 2002; Grocott et al. 2003); although modest auroral brightenings are associated with the flows (Milan et al. 2005b), the magnetic perturbation produced is small and so the significance of this phenomenon was not realized until radar measurements of the flows were available. These events have been termed “tail reconnection during IMF northwards, non-substorm intervals” or TRINNIs.

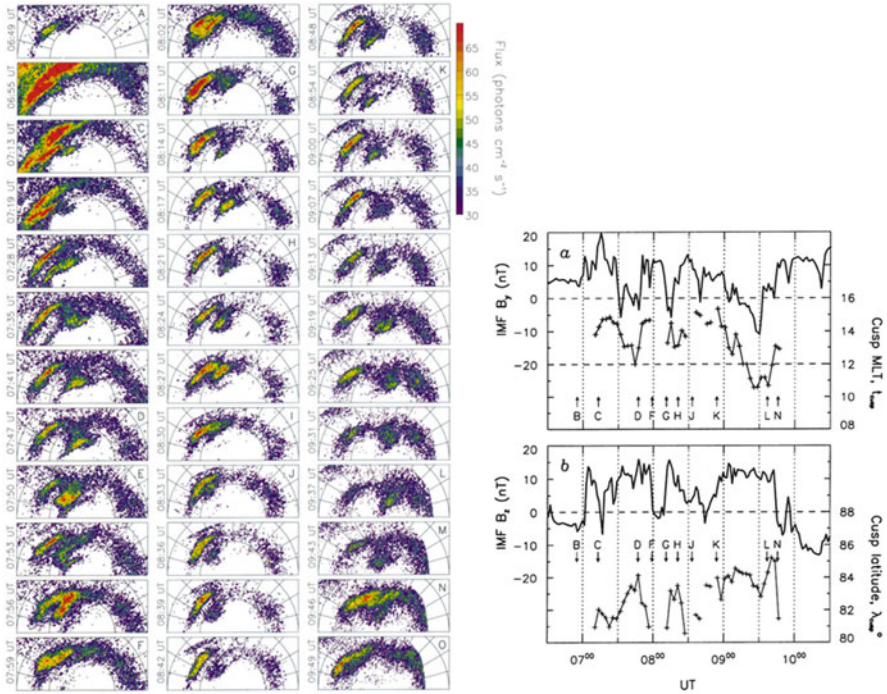


**Fig. 2.10** (Left) Observations of the dayside auroras from the Polar UVI instrument on 26 August 1998, showing the appearance of a cusp auroral spot poleward of the main auroral zone. (Right) The magnetic local time and latitude of the centroid of the cusp spot during this period, along with the corresponding IMF  $B_Y$  and  $B_Z$  components measured by the Wind spacecraft [from Milan et al. (2000)]

Grocott et al. (2004) demonstrated that the eastwards/westwards sense of the flows were associated with the  $B_Y$  component of the IMF, and postulated that they were driven by reconnection occurring in a magnetotail that is twisted by the tension forces imposed on lobe field lines interlinked with northwards IMF (e.g., Cowley 1981a). In this scenario, the flows should have opposite senses in the two hemispheres, subsequently verified by Grocott et al. (2005). Each TRINNI burst is thought to close  $\sim 0.1$  GWb of flux at a rate of 30 kV over a period of a few 10s min, compared to  $\sim 0.25$  GWb at  $\sim 100$  kV over an hour or more during substorms (Milan et al. 2007).

Another phenomenon associated with northwards IMF is the formation of theta auroras or transpolar arcs (TPAs), in which the polar cap becomes bisected by a tongue of auroras (Frank et al. 1982, 1986). These auroral features can form at the dawn or dusk sides of the polar cap, or appear to grow into the polar cap from the nightside auroral oval, and can subsequently move dawnwards or duskwards as IMF  $B_Y$  changes (Craven and Frank 1991; Craven et al. 1991; Cumnock et al. 1997; Cumnock and Blomberg 2004; Kullen 2000; Kullen et al. 2002; Fear and Milan 2012a). Several mechanisms for creating TPAs have been discussed in the

literature, but two main competing ideas gained ground, as discussed by Zhu et al. (1997). In the first, precipitation is associated with a field-aligned current sheet, which is itself associated with a large-scale shear in the ionospheric convection flow within the open polar cap (e.g., Burke et al. 1982). In the second, precipitation is associated with a tongue of closed field lines which protrudes into the polar cap from the nightside, effectively plasma sheet extending to much higher latitudes than usual (e.g., Frank et al. 1982). Milan et al. (2005b), Goudarzi et al. (2008) and Fear and Milan (2012b) demonstrated that TPA formation was sometimes associated with the occurrence of TRINNI flows, and proposed that the arc was associated with closed field lines that were created by reconnection in a twisted magnetotail and which could not easily convect to the dayside and so accumulated in the midnight sector, eventually protruding upwards into the lobes. This mechanism explains the observed local time dependence of TPA formation, dusk-side for IMF  $B_Y > 0$  and dawn-side for  $B_Y < 0$  in the northern hemisphere, due to the sense in the twist of the magnetotail. Subsequent motion of the arcs dawnwards or duskwards was postulated to be participation of these closed field lines embedded within the lobe in lobe stirring driven by single lobe reconnection (Milan et al. 2005b) or due to the asymmetrical addition of new open flux to the lobes by  $B_Y$ -dominated southwards IMF (Goudarzi et al. 2008).

## 2.8 Concluding Remarks

Dungey's open magnetosphere paradigm of magnetospheric dynamics provides a powerful theoretical framework within which to understand most aspects of the structure and large-scale dynamics of the magnetosphere. Observations of the expanding/contracting polar cap and the associated ionospheric convection pattern provide a means of quantitatively exploring magnetic reconnection rates, and the magnetospheric response to reconnection. Although the basic mechanisms are well-understood and placed on a firm observational footing, there are still several fundamental outstanding questions. It is not understood what leads to the onset of magnetotail reconnection during substorms. The role(s) of feedback loops within the coupled solar wind-magnetosphere-ionosphere system is (are) poorly understood: for instance, do heavy ion mass-loading of the plasma sheet or the magnetic perturbation produced by an enhanced ring current play a role in controlling magnetotail onset thresholds and rates?; do storm-time plasmaspheric plumes play a role in modulating the dayside reconnection rate through heavy ion mass-loading of the magnetopause? There is a significant body of work investigating mechanisms by which the transpolar voltage of the magnetosphere may saturate at values near  $\sim 250$  kV when solar wind driving is extreme, though there is perhaps a dearth of observations that allow this to be investigated in detail.

Two complementary pictures of magnetospheric dynamics exist. The ECPC describes dynamics in terms of changes in open flux and the stresses exerted by deviations of the magnetopause from hydrodynamic equilibrium with the solar

wind. Alternatively, the dynamics can be described in terms of the current systems that transmit stress throughout the magnetosphere. These two paradigms have yet to be fully reconciled, but new observational techniques to measure the spatial- and time-dependence of the currents allows their response in the context of the ECPC to be explored, and will allow the relationship between reconnection rates and FAC dynamics to be better understood.

This review has concentrated on the ramifications of the open model for the terrestrial magnetosphere, but magnetic reconnection clearly plays an important role in the magnetospheres of other planets. Although observational evidence is more difficult to acquire at Mercury or the outer planets, our understanding of the dynamics of those magnetospheres is indebted to the work of Dungey. We conclude by remarking that the Dungey cycle and ECPC (suitably modified for local conditions) have been invoked to explain behaviour at Mercury (e.g., Milan and Slavin 2011; Slavin et al. 2010), Jupiter (e.g., Cowley et al. 2003), Saturn (e.g., Badman et al. 2005; Cowley et al. 2005; Milan et al. 2005a), and Uranus (Cowley 2013). Inevitably, many exciting developments of Dungey's work will arise as observations of those distant systems improve.

**Acknowledgements** SEM was supported by the Science and Technology Facilities Council (STFC), UK, grant no. ST/K001000/1 and the Research Council of Norway/CoE under contract 223252/F50. SEM would like to thank the PIs of the instruments from which data are presented in this review article, including S. B. Mende of the University of California Berkeley (IMAGE FUV), G. K. Parks of the University of Washington (Polar UVI), B. J. Anderson of JHU/APL (AMPERE), and the PIs of the Super Dual Auroral Radar Network (SuperDARN). SuperDARN is a collection of radars funded by national scientific funding agencies of Australia, Canada, China, France, Japan, South Africa, United Kingdom and United States of America. SEM also thanks J. C. Coxon, of the University of Leicester, for producing Fig. 2.9 of this paper.

## References

- Akasofu, S.-I.: The development of the auroral substorm. *Planet. Space Sci.* **12**, 273–282 (1964)
- Akasofu, S.-I., Kamide, Y.: Substorm energy. *Planet. Space Sci.* **23**, 223 (1975)
- Akasofu, S.-I., Meng, C.-I., Marita, K.: Changes in the size of the open field line region during substorms. *Planet. Space Sci.* **40**, 1513–1524 (1992)
- Alcayde, D., Caudal, G., Fontanari, J.: Convection electric fields and electrostatic potential over  $61^\circ < \Lambda < 72^\circ$  invariant latitude observed with the European incoherent scatter facility. *J. Geophys. Res.* **91**, 233 (1986)
- Anderson, B.J., Takahashi, K., Toth, B.A.: Sensing global Birkeland currents with Iridium® engineering magnetometer data. *Geophys. Res. Lett.* **27**, 4045–4048 (2000). doi:[10.1029/2000GL000094](https://doi.org/10.1029/2000GL000094)
- Anderson, B.J., Takahashi, K., Kamei, T., Waters, C.L., Toth, B.A.: Birkeland current system key parameters derived from Iridium observations: method and initial validation results. *J. Geophys. Res.* **107**, 1079 (2002). doi:[10.1029/2001JA000080](https://doi.org/10.1029/2001JA000080)
- Aubry, M.P., Russell, C.T., Kivelson, M.G.: Inward motion of the magnetopause before a substorm. *J. Geophys. Res.* **75**, 7018–7031 (1970). doi:[10.1029/JA075i034p07018](https://doi.org/10.1029/JA075i034p07018)
- Badman, S.V., Bunce, E.J., Clarke, J.T., Cowley, S.W.H., Gérard, J.-C., Grodent, D., Milan, S.E.: Open flux estimates in Saturn's magnetosphere during the January 2004 Cassini-HST

- campaign, and implications for reconnection rates. *J. Geophys. Res.* **110**, A11216 (2005). doi:[10.1029/2005JA011240](https://doi.org/10.1029/2005JA011240)
- Baker, K.B., Dudeney, J.R., Greenwald, R.A., Pinnock, M., Newell, P.T., Rodger, A.S., Mattin, N., Meng, C.-I.: HF radar signatures of the cusp and low-latitude boundary layer. *J. Geophys. Res.* **100**, 7671–7695 (1995)
- Baker, D.N., Pulkkinen, T.I., Angelopoulos, V., Baumjohann, W., McPherron, R.L.: *J. Geophys. Res.* **101**, 12975–13010 (1996)
- Baker, K.B., Rodger, A.S., Lu, G.: HF-radar observations of the dayside magnetic merging rate: a geospace environment modeling boundary layer campaign study. *J. Geophys. Res.* **102**, 9603–9617 (1997)
- Belian, R.D., Cayton, T.E., Reeves, G.D.: Quasi-periodic global substorm-generated variations observed at geosynchronous orbit. In: Ashour-Abdalla, M., Chang, T., Dusenbury, P. (eds.) *Space Plasmas Coupling Between Small and Medium Scale Processes*. Geophysical Monograph Series, vol. 86, p. 143. AGU, Washington, DC (1995)
- Blanchard, G.T., Ellington, C.L., Lyons, L.R., Rich, F.J.: Incoherent scatter radar identification of the dayside magnetic separatrix and measurement of magnetic reconnection. *J. Geophys. Res.* **106**, 8185–8195 (2001)
- Boakes, P.D., Milan, S.E., Abel, G.A., Freeman, M.P., Chisham, G., Hubert, B., Sotirelis, T.: On the use of IMAGE FUV for estimating the latitude of the open/closed field line boundary in the ionosphere. *Ann. Geophys.* **26**, 2579–2769 (2008)
- Boakes, P.D., Milan, S.E., Abel, G.A., Freeman, M.P., Chisham, G., Hubert, B.: A statistical study of the open magnetic flux content of the magnetosphere at substorm onset. *Geophys. Res. Lett.* **36**, L04105 (2009). doi:[10.1029/2008GL037059](https://doi.org/10.1029/2008GL037059)
- Borovsky, J.E., Hesse, M., Birn, J., Kuznetsova, M.M.: What determines the reconnection rate at the dayside magnetosphere? *J. Geophys. Res.* **113**, A07210 (2008)
- Boudouridis, A., Zesta, E., Lyons, R., Anderson, P.C., Lummerzheim, D.: Effect of solar wind pressure pulses on the size and strength of the auroral oval. *J. Geophys. Res.* **108** (2003). doi:[10.1029/2002JA009373](https://doi.org/10.1029/2002JA009373)
- Brittnacher, M., Fillingim, M., Parks, G., Germany, G., Spann, J.: Polar cap area and boundary motion during substorms. *J. Geophys. Res.* **104**, 12251–12262 (1999)
- Burke, W.J., Gussenhoven, M.S., Kelley, M.C., Hardy, D.A., Rich, F.J.: Electric and magnetic field characteristics of discrete arcs in the polar cap. *J. Geophys. Res.* **87**, 2431–2443 (1982). doi:[10.1029/JA087iA04p02431](https://doi.org/10.1029/JA087iA04p02431)
- Burton, R.K., McPherron, R.L., Russell, C.T.: An empirical relationship between interplanetary conditions and Dst. *J. Geophys. Res.* **80**, 4204–4212 (1975)
- Caan, M.N., McPherron, R.L., Russell, C.T.: The statistical magnetic signature of magnetospheric substorms. *Planet. Space Sci.* **26**, 269–279 (1978)
- Cai, X., Clauer, C.R., Ridley, A.J.: Statistical analysis of ionospheric potential patterns for isolated substorms and sawtooth events. *Ann. Geophys.* **24**, 1977–1991 (2006)
- Cai, X., Zhang, J.-C., Clauer, C.R., Liemohn, M.W.: Relationship between sawtooth events and magnetic storms. *J. Geophys. Res.* **116**, A07208 (2011). doi:[10.1029/2010JA016310](https://doi.org/10.1029/2010JA016310)
- Chisham, G., Lester, M., Milan, S.E., Freeman, M.P., Bristow, W.A., Grocott, A., McWilliams, K. A., Ruohoniemi, J.M., Yeoman, T.K., Dyson, P.L., Greenwald, R.A., Kikuchi, T., Pinnock, M., Rash, J.P.S., Sato, N., Sofko, G.J., Villain, J.-P., Walker, A.D.M.: A decade of the Super Dual Auroral Radar Network (SuperDARN): scientific achievements, new techniques and future directions. *Surv. Geophys.* **28**, 33–109 (2007). doi:[10.1007/s10712-007-9017-8](https://doi.org/10.1007/s10712-007-9017-8)
- Chisham, G., Freeman, M.P., Abel, G.A., Lam, M.M., Pinnock, M., Coleman, I.J., Milan, S.E., Lester, M., Bristow, W.A., Greenwald, R.A., Sofko, G.J., Villain, J.-P.: Remote sensing of the spatial and temporal structure of magnetopause and magnetotail reconnection from the ionosphere. *Rev. Geophys.* **46**, RG1004 (2008). doi:[10.1029/2007RG000223](https://doi.org/10.1029/2007RG000223)
- Clausen, L.B.N., Baker, J.B.H., Ruohoniemi, J.M., Milan, S.E., Anderson, B.J.: Dynamics of the region 1 Birkeland current oval derived from the Active Magnetosphere and Planetary

- Electrodynamics Response Experiment (AMPERE). *J. Geophys. Res.* **117**, A06233 (2012). doi:[10.1029/2012JA017666](https://doi.org/10.1029/2012JA017666)
- Clausen, L.B.N., Baker, J.B.H., Ruohoniemi, J.M., Milan, S.E., Coxon, J.C., Wing, S., Ohtani, S., Anderson, B.J.: Temporal and spatial dynamics of the region 1 and 2 Birkeland currents during substorms. *J. Geophys. Res. Space Phys.* **118**, 3007–3016 (2013a). doi:[10.1002/jgra.50288](https://doi.org/10.1002/jgra.50288)
- Clausen, L.B.N., Milan, S.E., Baker, J.B.H., Ruohoniemi, J., Glassmeier, K.-H., Coxon, J.C., Anderson, B.J.: On the influence of open magnetic flux on substorm intensity: ground- and space-based observations. *J. Geophys. Res. Space Phys.* **118**, 2958–2969 (2013b). doi:[10.1002/jgra.50308](https://doi.org/10.1002/jgra.50308)
- Cooling, B.M.A., Owen, C.J., Schwartz, S.J.: Role of magnetosheath flow in determining the motion of open flux tubes. *J. Geophys. Res.* **106**, 18763–18775 (2001)
- Coroniti, F.V., Kennel, C.F.: Changes in magnetospheric configuration during the substorm growth phase. *J. Geophys. Res.* **77**, 3361–3370 (1972). doi:[10.1029/JA077i019p03361](https://doi.org/10.1029/JA077i019p03361)
- Coumans, V., Blockx, C., Gérard, J.-C., Hubert, B., Connors, M.: Global morphology of substorm growth phases observed by the IMAGES12 imager. *J. Geophys. Res.* **112**, A11211 (2007). doi:[10.1029/2007JA012329](https://doi.org/10.1029/2007JA012329)
- Cowley, S.W.H.: Magnetospheric asymmetries associated with the Y-component of the IMF. *Planet. Space Sci.* **29**, 79–96 (1981)
- Cowley, S.W.H.: Magnetospheric and ionospheric flow and the interplanetary magnetic field. In: *The Physical Basis of the Ionosphere in the Solar-Terrestrial System*, AGARD-CP-295, pp. (4–1)–(4–14) (1981b)
- Cowley, S.W.H.: The structure and length of tail-associated phenomena in the solar wind downstream from the Earth. *Planet. Space Sci.* **7**, 1039 (1991)
- Cowley, S.W.H.: Magnetosphere-ionosphere interactions: a tutorial review. In: Ohtani, S., et al. (eds.) *Magnetospheric Current Systems*. Geophysical Monograph Series, vol. 118, pp. 91–106. AGU, Washington, DC (2000). doi:[10.1029/GM118p0091](https://doi.org/10.1029/GM118p0091)
- Cowley, S.W.H.: Response of Uranus' auroras to solar wind compressions at equinox. *J. Geophys. Res. Space Phys.* **118**, 2897–2902 (2013). doi:[10.1002/jgra.50323](https://doi.org/10.1002/jgra.50323)
- Cowley, S.W.H., Lockwood, M.: Excitation and decay of solar wind-driven flows in the magnetosphere-ionosphere system. *Ann. Geophys.* **10**, 103–115 (1992)
- Cowley, S.W.H., Owen, C.J.: A simple illustrative model of open flux tube motion over the dayside magnetopause. *Planet. Space Sci.* **27**, 1461–1475 (1989)
- Cowley, S.W.H., Bunce, E.J., Stallard, T.S., Miller, S.: Jupiter's polar ionospheric flows: theoretical interpretation. *Geophys. Res. Lett.* **30**, 1220 (2003). doi:[10.1029/2002GL016030](https://doi.org/10.1029/2002GL016030)
- Cowley, S.W.H., Badman, S.V., Bunce, E.J., Clarke, J.T., Gérard, J.-C., Grodent, D., Jackman, C. M., Milan, S.E., Yeoman, T.K.: Reconnection in a rotation-dominated magnetosphere and its relation to Saturn's auroral dynamics. *J. Geophys. Res.* **110**, A02201 (2005). doi:[10.1029/2004JA010796](https://doi.org/10.1029/2004JA010796)
- Craven, J.D., Frank, L.A.: Latitudinal motions of the aurora during substorms. *J. Geophys. Res.* **92**, 4565 (1987)
- Craven, J.D., Frank, L.A.: Diagnosis of auroral dynamics using global auroral imaging with emphasis on large-scale evolution. In: Meng, C.-I., Rycroft, M.J., Frank, L.A. (eds.) *Auroral Physics*, pp. 273–288. Cambridge University Press, Cambridge, UK (1991)
- Craven, J.D., Murphree, J.S., Frank, L.A., Cogger, L.L.: Simultaneous optical observations of transpolar arcs in the two polar caps. *Geophys. Res. Lett.* **18**, 2297–2300 (1991). doi:[10.1029/91GL02308](https://doi.org/10.1029/91GL02308)
- Cumnock, J.A., Blomberg, L.G.: Transpolar arc evolution and associated potential patterns. *Ann. Geophys.* **22**, 1213–1231 (2004). doi:[10.5194/angeo-22-1213-2004](https://doi.org/10.5194/angeo-22-1213-2004)
- Cumnock, J.A., Sharber, J.R., Heelis, R.A., Hairston, M.R., Craven, J.D.: Evolution of the global aurora during positive IMF  $B_Z$  and varying IMF  $B_Y$  conditions. *J. Geophys. Res.* **102**, 17489–17497 (1997). doi:[10.1029/97JA01182](https://doi.org/10.1029/97JA01182)
- de la Beaujardiere, O., Lyons, L.R., Friis-Christensen, E.: Sondrestrom radar measurements of the reconnection electric field. *J. Geophys. Res.* **96**, 13907–13912 (1991)

- DeJong, A.D., Clauer, C.R.: Polar UVI images to study steady magnetospheric convection events: initial results. *Geophys. Res. Lett.* **32**, L24101 (2005). doi:[10.1029/2005GL024498](https://doi.org/10.1029/2005GL024498)
- DeJong, A.D., Cai, X., Clauer, R.C., Spann, J.F.: Aurora and open magnetic flux during isolated substorms, sawteeth, and SMC events. *Ann. Geophys.* **25**, 1865–1876 (2007)
- DeJong, A.D., Ridley, A.J., Clauer, C.R.: Balanced reconnection intervals: four case studies. *Ann. Geophys.* **26**, 3897–3912 (2008)
- Dungey, J.W.: Interplanetary magnetic fields and the auroral zones. *Phys. Rev. Lett.* **6**, 47–48 (1961)
- Dungey, J.W.: The structure of the ionosphere, or adventures in velocity space. In: DeWitt, C., Hiebolt, J., Lebeau, A. (eds.) *Geophysics: The Earth's Environment*, pp. 526–536. Gordon and Breach, New York (1963)
- Dungey, J.W.: The length of the magnetospheric tail. *J. Geophys. Res.* **70**, 1753 (1965)
- Emmedi, A., Cowley, S.W.H., Lockwood, M., Bromage, B.J.I., Willis, D.M., Luhr, H.: The dependence of high-latitude dayside ionospheric flows on the north-south component of the IMF—a high time resolution correlation-analysis using EISCAT POLAR and AMPTE UKS and IRM data. *Planet. Space Sci.* **36**, 471–498 (1988)
- Evans, J.V., Holt, J.M., Oliver, W.L., Wand, R.H.: Millstone Hill incoherent scatter observations of auroral convection over  $60^\circ < \Lambda < 75^\circ$ , 2, Initial results. *J. Geophys. Res.* **85**, 41 (1980)
- Fear, R.C., Milan, S.E.: The IMF dependence of the local time of transpolar arcs: implications for formation mechanism. *J. Geophys. Res.* **117**, A03213 (2012a). doi:[10.1029/2011JA017209](https://doi.org/10.1029/2011JA017209)
- Fear, R.C., Milan, S.E.: Ionospheric flows relating to transpolar arc formation. *J. Geophys. Res.* **117**, A09230 (2012b). doi:[10.1029/2012JA017830](https://doi.org/10.1029/2012JA017830)
- Foster, J.C.: An empirical electric field model derived from Chatanika radar data. *J. Geophys. Res.* **88**, 981 (1983)
- Frank, L.A., Craven, J.D.: Imaging results from Dynamics Explorer 1. *Rev. Geophys.* **26**, 249 (1988)
- Frank, L.A., Craven, J.D., Burch, J.L., Winningham, J.D.: Polar views of the Earth's aurora with Dynamics Explorer. *Geophys. Res. Lett.* **9**, 1001–1004 (1982)
- Frank, L.A., Craven, J.D., Gurnett, D.A., Shawhan, S.D., Weimer, D.R., Burch, J.L., Winningham, J.D., Chappell, C.R., Waite, J.H., Heelis, R.A., Maynard, N.C., Sugiura, M., Peterson, W.K., Shelley, E.G.: The theta aurora. *J. Geophys. Res.* **91**, 3177–3224 (1986)
- Freeman, M.P.: A unified model of the response of ionospheric convection to changes in the interplanetary field. *J. Geophys. Res.* **108**, 1024 (2003). doi:[10.1029/2002JA009385](https://doi.org/10.1029/2002JA009385)
- Freeman, M.P., Southwood, D.J.: The effect of magnetospheric erosion on mid- and high-latitude ionospheric flows. *Planet. Space Sci.* **36**, 509–522 (1988)
- Frey, H.U., Mende, S.B., Immel, T.J., Fuselier, S.A., Claffin, E.S., Gerard, J.C., Hubert, B.: Proton aurora in the cusp. *J. Geophys. Res.* **107**, 1091 (2002). doi:[10.1029/2001JA900161](https://doi.org/10.1029/2001JA900161)
- Frey, H.U., Mende, S.B., Angelopoulos, V., Donovan, E.F.: Substorm onset observations by IMAGE-FUV. *J. Geophys. Res.* **109**, 2004 (2004). doi:[10.1029/2004JA010607](https://doi.org/10.1029/2004JA010607)
- Goudarzi, A., Lester, M., Milan, S.E., Frey, H.U.: Multi-instrument observations of a transpolar arc in the northern hemisphere. *Ann. Geophys.* **26**, 201–210 (2008)
- Greenwald, R.A., Weiss, W., Nielsen, E., Thomson, N.R.: STARE: a new radar auroral backscatter experiment in northern Scandinavia. *Radio Sci.* **13**, 1021–1039 (1978). doi:[10.1029/RS013i006p01021](https://doi.org/10.1029/RS013i006p01021)
- Greenwald, R.A., Baker, K.B., Dudeney, J.R., Pinnock, M., Jones, T.B., Thomas, E.C., Villain, J.-P., Cerisier, J.-C., Senior, C., Hanuise, C., Hunsucker, R.D., Sofko, G., Koehler, J., Nielsen, E., Pellinen, R., Walker, A.D.M., Sato, N., Yamagishi, H.: DARN/SuperDARN: a global view of the dynamics of high-latitude convection. *Space Sci. Rev.* **71**, 761–796 (1995)
- Grocott, A., Cowley, S.W.H., Sigwarth, J.B.: Ionospheric flow during extended intervals of northward but By-dominated IMF. *Ann. Geophys.* **21**, 509–538 (2003)
- Grocott, A., Badman, S.V., Cowley, S.W.H., Yeoman, T.K., Cripps, P.J.: The influence of IMF  $B_y$  on the nature of the nightside high latitude ionospheric flow during intervals of positive IMF  $B_z$ . *Ann. Geophys.* **22**, 1755–1764 (2004)

- Grocott, A., Yeoman, T.K., Milan, S.E., Cowley, S.W.H.: Interhemispheric observations of the ionospheric signature of tail reconnection during IMF-northward non-substorm intervals. *Ann. Geophys.* **23**, 1763–1770 (2005)
- Grocott, A., Wild, J.A., Milan, S.E., Yeoman, T.K.: Superposed epoch analysis of the ionospheric convection evolution during substorms: onset latitude dependence. *Ann. Geophys.* **27**, 591–600 (2009)
- Haerendel, G., Paschmann, G., Scokopke, N., Rosenbauer, H., Hedgecock, P.C.: The frontside boundary layer of the magnetosphere and the problem of reconnection. *J. Geophys. Res.* **83**, 3195 (1978)
- Hairston, M.R., Hill, T.W., Heelis, R.A.: Observed saturation of the ionospheric polar cap potential during the 31 March 2001 storm. *Geophys. Res. Lett.* **30**, 1325 (2003). doi:[10.1029/2002GL015894](https://doi.org/10.1029/2002GL015894)
- Hairston, M.R., Drake, K.A., Skoug, R.: Saturation of the ionospheric polar cap potential during the October–November 2003 superstorms. *J. Geophys. Res.* **110**, A09S26 (2005). doi:[10.1029/2004JA010864](https://doi.org/10.1029/2004JA010864)
- Heppner, J.P.: Empirical models of high-latitude electric fields. *J. Geophys. Res.* **82**, 1115 (1977)
- Heppner, J.P., Maynard, N.C.: Empirical high-latitude electric-field models. *J. Geophys. Res.* **92**, 4467–4489 (1987)
- Holzer, R.E., Slavin, J.A.: Magnetic-flux transfer associated with expansions and contractions of dayside magnetosphere. *J. Geophys. Res.* **83**, 3831–3839 (1978)
- Holzer, R.E., Slavin, J.A.: A correlative study of magnetic flux transfer in the magnetosphere. *J. Geophys. Res.* **84**, 2573–2578 (1979)
- Hsu, T.-S., McPherron, R.L.: An evaluation of the statistical significance of the association between northward turnings of the interplanetary magnetic field and substorm expansion onsets. *J. Geophys. Res.* **107**, 1398 (2002). doi:[10.1029/2000JA000125](https://doi.org/10.1029/2000JA000125)
- Huang, C.-S.: Evidence of periodic (2–3 hour) near-tail magnetic reconnection and plasmoid formation: geotail observations. *Geophys. Res. Lett.* **29**, 2189 (2002). doi:[10.1029/2002GL016162](https://doi.org/10.1029/2002GL016162)
- Huang, C.-S., Sofko, G.J., Koustov, A.V., Andre, D.A., Ruohoniemi, J.M., Greenwald, R.A., Hairston, M.R.: Evolution of ionospheric multicell convection during northward interplanetary magnetic field with  $|B_x/B_y| > 1$ . *J. Geophys. Res.* **105**, 27095–27107 (2000)
- Huang, C.-S., DeJong, A.D., Cai, X.: Magnetic flux in the magnetotail and polar cap during sawteeth, isolated substorms, and steady magnetospheric convection events. *J. Geophys. Res.* **114**, A07202 (2009). doi:[10.1029/2009JA014232](https://doi.org/10.1029/2009JA014232)
- Hubert, B., Milan, S.E., Grocott, A., Cowley, S.W.H., Gérard, J.-C.: Dayside and nightside reconnection rates inferred from IMAGE-FUV and SuperDARN data. *J. Geophys. Res.* **111**, A03217 (2006a). doi:[10.1029/2005JA011140](https://doi.org/10.1029/2005JA011140)
- Hubert, B., Palmroth, M., Laitinen, T.V., Janhunen, P., Milan, S.E., Grocott, A., Cowley, S.W.H., Pulkkinen, T., Gérard, J.-C.: Compression of the Earth's magnetotail by interplanetary shocks drives magnetic flux closure. *Geophys. Res. Lett.* **33**, L10105 (2006b). doi:[10.1029/2006GL026008](https://doi.org/10.1029/2006GL026008)
- Hubert, B., Milan, S.E., Grocott, A., Cowley, S.W.H., Gérard, J.C.: Open magnetic flux and magnetic flux closure during sawtooth events. *Geophys. Res. Lett.* **35**, L23301 (2008). doi:[10.1029/2008GL036374](https://doi.org/10.1029/2008GL036374)
- Hubert, B., Blockx, C., Milan, S.E., Cowley, S.W.H.: Statistical properties of flux closure induced by solar wind dynamic pressure fronts. *J. Geophys. Res.* **114**, A07211 (2009). doi:[10.1029/2008JA013813](https://doi.org/10.1029/2008JA013813)
- Iijima, T., Potemra, T.A.: Large-scale characteristics of field-aligned currents associated with substorms. *J. Geophys. Res.* **83**, 599 (1978)
- Imber, S.M., Milan, S.E., Hubert, B.: Ionospheric flow and auroral signatures of dual lobe reconnection. *Ann. Geophys.* **24**, 3115–3129 (2006)
- Imber, S.M., Milan, S.E., Hubert, B.: Observations of significant flux closure by dual lobe reconnection. *Ann. Geophys.* **25**, 1617–1627 (2007)

- Imber, S.M., Milan, S.E., Lester, M.: The SuperDARN Heppner-Maynard Boundary as a proxy for the latitude of the auroral oval. *J. Geophys. Res. Space Phys.* **118**, 685–697 (2013a). doi:[10.1029/2012JA018222](https://doi.org/10.1029/2012JA018222)
- Imber, S.M., Milan, S.E., Lester, M.: Solar cycle variations in polar cap area measured by the SuperDARN radars. *J. Geophys. Res. Space Phys.* **118**, 6188–6196 (2013b). doi:[10.1002/jgra.50509](https://doi.org/10.1002/jgra.50509)
- Juusola, L., Partamies, N., Tanskanen, E.: Effect of the ring current on preconditioning the magnetosphere for steady magnetospheric convection. *Geophys. Res. Lett.* **40**, 1917–1921 (2013). doi:[10.1002/grl.50405](https://doi.org/10.1002/grl.50405)
- Kamide, Y., Kokubun, S., Bargatze, L.F., Frank, L.A.: The size of the polar cap as an indicator of substorm energy. *Phys. Chem. Earth C* **24**, 119 (1999)
- Kissinger, J., McPherron, R.L., Hsu, T.-S., Angelopoulos, V., Chu, X.: Necessity of substorm expansions in the initiation of steady magnetospheric convection. *Geophys. Res. Lett.* **39**, L15105 (2012a). doi:[10.1029/2012GL052599](https://doi.org/10.1029/2012GL052599)
- Kissinger, J., McPherron, R.L., Hsu, T.-S., Angelopoulos, V.: Diversion of plasma due to high pressure in the inner magnetosphere during steady magnetospheric convection. *J. Geophys. Res.* **117**, A05206 (2012b). doi:[10.1029/2012JA017579](https://doi.org/10.1029/2012JA017579)
- Kistler, L.M., Moukikis, C.G., Cao, X., Frey, H., Klecker, B., Dandouras, I., Korth, A., Marcucci, M.F., Lundin, R., McCarthy, M., Friedel, R., Lucek, E.: Ion composition and pressure changes in storm time and nonstorm substorms in the vicinity of the near-Earth neutral line. *J. Geophys. Res.* **111**, A11222 (2006). doi:[10.1029/2006JA011939](https://doi.org/10.1029/2006JA011939)
- Kullen, A.: The connection between transpolar arcs and magnetotail rotation. *Geophys. Res. Lett.* **27**, 73–76 (2000). doi:[10.1029/1999GL010675](https://doi.org/10.1029/1999GL010675)
- Kullen, A., Brittnacher, M., Cumnock, J.A., Blomberg, L.G.: Solar wind dependence of the occurrence and motion of polar auroral arcs: a statistical study. *J. Geophys. Res.* **107**, 1362 (2002). doi:[10.1029/2002JA009245](https://doi.org/10.1029/2002JA009245)
- Lester, M., Milan, S.E., Besser, V., Smith, R.: A case study of HF radar spectra and 630.0 nm auroral emission. *Ann. Geophys.* **19**, 327–340 (2001)
- Lewis, R.V., Freeman, M.P., Reeves, G.D.: The relationship of HF backscatter to the accumulation of open magnetic flux prior to substorm onset. *J. Geophys. Res.* **103**, 26613–26619 (1998)
- Lockwood, M.: On flow reversal boundaries and transpolar voltage in average models of high-latitude convection. *Planet. Space Sci.* **39**, 397–409 (1991)
- Lockwood, M., Freeman, M.P.: Recent ionospheric observations relating to solar wind-magnetosphere coupling. *Philos. Trans. R. Soc. Lond. A.* **328**, 93 (1989)
- Lockwood, M., Cowley, S.W.H., Freeman, M.P.: The excitation of plasma convection in the high-latitude ionosphere. *J. Geophys. Res.* **95**, 7961–7972 (1990)
- Lockwood, M., Cowley, S.W.H.: Ionospheric convection and the substorm cycle. In: *Proceedings of the International Conference on Substorms (ICS-1)*, ESA SP-335, pp. 99–109 (1992)
- Lockwood, M., Hairston, M., Finch, I., Rouillard, A.: Transpolar voltage and polar cap flux during the substorm cycle and steady convection events. *J. Geophys. Res.* **114**, A01210 (2009). doi:[10.1029/2008JA013697](https://doi.org/10.1029/2008JA013697)
- Lyons, L.R., Blanchard, G.T., Samson, J.C., Lepping, R.P., Yamamoto, T., Moretto, T.: Coordinated observations demonstrating external substorm triggering. *J. Geophys. Res.* **102**, 27039–27051 (1997)
- Marcucci, M.F., Coco, I., Ambrosino, D., Amata, E., Milan, S.E., Bavassano Cattaneo, M.B., Retinò, A.: Extended SuperDARN and IMAGE observations for northward IMF: evidence for dual lobe reconnection. *J. Geophys. Res.* **113**, A02204 (2008). doi:[10.1029/2007JA012466](https://doi.org/10.1029/2007JA012466)
- McPherron, R.L.: Growth phase of magnetospheric substorms. *J. Geophys. Res.* **75**, 5592–5599 (1970)
- McWilliams, K.A., Pfeifer, J.B., McPherron, R.L.: Steady magnetospheric convection selection criteria: implications of global SuperDARN convection measurements. *Geophys. Res. Lett.* **35**, L09102 (2008)

- Mende, S.B., Heeterdks, H., Frey, H.U., Lampton, M., Geller, S.P., Habraken, S., Renotte, E., Jamar, C., Rochus, P., Spann, J., Fuselier, S.A., Gerard, J.-C., Gladstone, R., Murphree, S., Cogger, L.: Far ultraviolet imaging from the IMAGE spacecraft. 1. System design. *Space Sci. Rev.* **91**, 243–270 (2000a)
- Mende, S.B., Heeterdks, H., Frey, H.U., Lampton, M., Geller, S.P., Abiad, R., Siegmund, O.H.W., Tremsin, A.S., Spann, J., Dougani, H., Fuselier, S.A., Magoncelli, A.L., Bumala, M.B., Murphree, S., Trondsen, T.: Far ultraviolet imaging from the IMAGE spacecraft. 2. Wideband FUV imaging. *Space Sci. Rev.* **91**, 271–285 (2000b)
- Meng, C.-I., Holzworth, R.H., Akasofu, S.-I.: Auroral circle: delineating the poleward boundary of the quiet auroral belt. *J. Geophys. Res.* **82**, 164 (1977)
- Milan, S.E.: A simple model of the flux content of the distant magnetotail. *J. Geophys. Res.* **109**, A07210 (2004a). doi:[10.1029/2004JA010397](https://doi.org/10.1029/2004JA010397)
- Milan, S.E.: Dayside and nightside contributions to the cross polar cap potential: placing an upper limit on a viscous-like interaction. *Ann. Geophys.* **22**, 3771–3777 (2004b)
- Milan, S.E.: Both solar wind-magnetosphere coupling and ring current intensity control of the size of the auroral oval. *Geophys. Res. Lett.* **36**, L18101 (2009). doi:[10.1029/2009GL039997](https://doi.org/10.1029/2009GL039997)
- Milan, S.E.: Modelling Birkeland currents in the expanding/contracting polar cap paradigm. *J. Geophys. Res.* **118**, 5532–5542 (2013). doi:[10.1002/jgra.50393](https://doi.org/10.1002/jgra.50393)
- Milan, S.E., Slavin, J.A.: An assessment of the length and variability of Mercury’s magnetotail. *Planet. Space Sci.* **59**, 2048–2065 (2011). doi:[10.1016/j.pss.2001.05.007](https://doi.org/10.1016/j.pss.2001.05.007)
- Milan, S.E., Lester, M., Cowley, S.W.H., Brittnacher, M.: Dayside convection and auroral morphology during an interval of northward interplanetary magnetic field. *Ann. Geophys.* **18**, 436–444 (2000)
- Milan, S.E., Lester, M., Cowley, S.W.H., Oksavik, K., Brittnacher, M., Greenwald, R.A., Sofko, G., Villain, J.-P.: Variations in polar cap area during two substorm cycles. *Ann. Geophys.* **21**, 1121–1140 (2003)
- Milan, S.E., Cowley, S.W.H., Lester, M., Wright, D.M., Slavin, J.A., Fillingim, M., Singer, H.J.: Response of the magnetotail to changes in the open flux content of the magnetosphere. *J. Geophys. Res.* **109**, A04220 (2004). doi:[10.1029/2003JA010350](https://doi.org/10.1029/2003JA010350)
- Milan, S.E., Bunce, E.J., Cowley, S.W.H., Jackman, C.M.: Implications of rapid planetary rotation for the Dungey magnetotail of Saturn. *J. Geophys. Res.* **110**, A03209 (2005a). doi:[10.1029/2004JA010716](https://doi.org/10.1029/2004JA010716)
- Milan, S.E., Hubert, B., Grocott, A.: Formation and motion of a transpolar arc in response to dayside and nightside reconnection. *J. Geophys. Res.* **110**, A01212 (2005b). doi:[10.1029/2004JA010835](https://doi.org/10.1029/2004JA010835)
- Milan, S.E., Wild, J.A., Hubert, B., Carr, C.M., Lucek, E.A., Bosqued, J.M., Watermann, J.F., Slavin, J.A.: Flux closure during a substorm observed by Cluster, Double Star, IMAGE FUV, SuperDARN, and Greenland magnetometers. *Ann. Geophys.* **24**, 751–767 (2006)
- Milan, S.E., Provan, G., Hubert, B.: Magnetic flux transport in the Dungey cycle: a survey of dayside and nightside reconnection rates. *J. Geophys. Res.* **112**, A01209 (2007). doi:[10.1029/2006JA011642](https://doi.org/10.1029/2006JA011642)
- Milan, S.E., Boakes, P.D., Hubert, B.: Response of the expanding/contracting polar cap to weak and strong solar wind driving: implications for substorm onset. *J. Geophys. Res.* **113**, A09215 (2008). doi:[10.1029/2008JA013340](https://doi.org/10.1029/2008JA013340)
- Milan, S.E., Grocott, A., Forsyth, C., Imber, S.M., Boakes, P.D., Hubert, B.: A superposed epoch analysis of auroral evolution during substorm growth, onset and recovery: open magnetic flux control of substorm intensity. *Ann. Geophys.* **27**, 659–668 (2009a)
- Milan, S.E., Hutchinson, J., Boakes, P.D., Hubert, B.: Influences on the radius of the auroral oval. *Ann. Geophys.* **27**, 2913–2924 (2009b)
- Milan, S.E., Gosling, J.S., Hubert, B.: Relationship between interplanetary parameters and the magnetopause reconnection rate quantified from observations of the expanding polar cap. *J. Geophys. Res.* **117** (2012). doi:[10.1029/2011JA017082](https://doi.org/10.1029/2011JA017082)

- Morelli, J.P., Bunting, R.J., Cowley, S.W.H., Farrugia, C.J., Freeman, M.P., Friis-Christensen, E., Jones, G.O.L., Lester, M., Lewis, R.V., Luhr, H., Orr, D., Pinnock, M., Reeves, G.D., Williams, P.J.S., Yeoman, T.K.: Radar observations of auroral zone flows during a multiple-onset substorm. *Ann. Geophys.* **13**, 1144–1163 (1995)
- Morley, S.K., Freeman, M.P.: On the association between northward turnings of the interplanetary magnetic field and substorm onsets. *Geophys. Res. Lett.* **34**, L08104 (2007). doi:[10.1029/2006GL028891](https://doi.org/10.1029/2006GL028891)
- Øieroset, M., Raeder, J., Phan, T.D., Wing, S., McFadden, J.P., Li, W., Fujimoto, M., Rème, H., Balogh, A.: Global cooling and densification of the plasma sheet during an extended period of purely Northward IMF on October 22–24, 2003. *Geophys. Res. Lett.* **32**, L12S07 (2005). doi:[10.1029/2004GL021523](https://doi.org/10.1029/2004GL021523)
- Ouellette, J.E., Brambles, O.J., Lyon, J.G., Lotko, W., Rogers, B.N.: Properties of outflow-driven sawtooth substorms. *J. Geophys. Res. Space Phys.* **118**, 3223–3232 (2013). doi:[10.1002/jgra.50309](https://doi.org/10.1002/jgra.50309)
- Partamies, N., Pulkkinen, T.I., McPherron, R.L., McWilliams, K., Bryant, C.R., Tanskanen, E., Singer, H.J., Reeves, G.D., Thomsen, M.F.: Statistical survey on sawtooth events, SMCs and isolated substorms. *Adv. Space Res.* **44**, 376 (2009). doi:[10.1016/j.asr.2009.03.013](https://doi.org/10.1016/j.asr.2009.03.013)
- Petrinec, S.M., Russell, C.T.: Near-Earth magnetotail shape and size as determined from the magnetopause flaring angle. *J. Geophys. Res.* **101**, 137–152 (1996)
- Reiff, P.H., Spiro, R.W., Hill, T.W.: Dependence of polar cap potential drop on interplanetary parameters. *J. Geophys. Res.* **86**, 7639–7648 (1981)
- Rich, F.J., Hairston, M.: Large-scale convection patterns observed by DMSP. *J. Geophys. Res.* **99**, 3827–3844 (1994)
- Rostoker, G., Akasofu, S.-I., Foster, J., Greenwald, R.A., Kamide, Y., Kawasaki, K., Lui, A.T.Y., McPherron, R.L., Russell, C.T.: Magnetospheric substorms—definition and signatures. *J. Geophys. Res.* **85**, 1663–1668 (1980)
- Ruohoniemi, J.M., Greenwald, R.A.: Statistical patterns of high-latitude convection obtained from Goose Bay HF radar observations. *J. Geophys. Res.* **101**, 21743–21763 (1996)
- Senior, C., Cerisier, J.-C., Rich, F., Lester, M., Parks, G.K.: Strong sunward propagating flow bursts in the night sector during quiet solar wind conditions, SuperDARN and satellite observations. *Ann. Geophys.* **20**, 771–779 (2002)
- Sergeev, V.A.: On the state of the magnetosphere during prolonged periods of southward oriented IMF. *Phys. Solariterr. Potsdam* **5**, 39 (1977)
- Shepherd, S.G.: Polar cap potential saturation: observations, theory, and modelling. *J. Atmos. Sol. Terr. Phys.* **69**, 234–248 (2006)
- Shukhtina, M.A., Dmitrieva, N.P., Popova, N.G., Sergeev, V.A., Yahnin, A.G., Despirak, I.V.: Observational evidence of the loading-unloading substorm scheme. *Geophys. Res. Lett.* **32**, L17107 (2005). doi:[10.1029/2005GL023779](https://doi.org/10.1029/2005GL023779)
- Shukhtina, M.A., Sergeev, V.A., DeJong, A.D., Hubert, B.: Comparison of magnetotail magnetic flux estimates based on global auroral images and simultaneous solar wind-magnetotail measurements. *J. Atmos. Sol. Terr. Phys.* **72**, 1282–1291 (2010). doi:[10.1016/j.jastp.2010.09.013](https://doi.org/10.1016/j.jastp.2010.09.013)
- Siscoe, G.L., Huang, T.S.: Polar cap inflation and deflation. *J. Geophys. Res.* **90**, 543–547 (1985)
- Siscoe, G.L., Crooker, N.U., Siebert, K.D.: Transpolar potential saturation: roles of region 1 current system and solar wind ram pressure. *J. Geophys. Res.* **107**, 1321 (2002). doi:[10.1029/2001JA009176](https://doi.org/10.1029/2001JA009176)
- Siscoe, G., Raeder, J., Ridley, A.J.: Transpolar potential saturation models compared. *J. Geophys. Res.* **109**, A09203 (2004). doi:[10.1029/2003JA010318](https://doi.org/10.1029/2003JA010318)
- Slavin, J.A., Fairfield, D.H., Lepping, R.P., Hesse, M., Ieda, A., Tanskanen, E., Østgaard, N., Mukai, T., Nagai, T., Singer, H.J., Sutcliffe, P.R.: Simultaneous observations of earthward flow bursts and plasmoid ejection during magnetospheric substorms. *J. Geophys. Res.* **107**(A7), 1106 (2002). doi:[10.1029/2000JA003501](https://doi.org/10.1029/2000JA003501)

- Slavin, J.A., Anderson, B.J., Baker, D.N., Benna, M., Boardsen, S.A., Gloeckler, G., Gold, R.E., Ho, G.C., Korth, H., Krimigis, S.M., McNutt Jr., R.L., Nittler, L.R., Raines, J.M., Sarantos, M., Schriver, D., Solomon, S.C., Starr, R.D., Trávníček, P.M., Zurbuchen, T.H.: MESSENGER observations of extreme loading and unloading of Mercury's magnetic tail. *Science* **329**, 655 (2010). doi:[10.1126/science.1188067](https://doi.org/10.1126/science.1188067)
- Taylor, J.R., Yeoman, T.K., Lester, M., Emery, B.A., Knipp, D.J.: Variations in the polar cap area during intervals of substorm activity on 20–21 March 1990 deduced from AMIE convection maps. *Ann. Geophys.* **14**, 879–887 (1996)
- Wild, J.A., Woodfield, E.E., Morley, S.K.: On the triggering of auroral substorms by northward turnings of the interplanetary magnetic field. *Ann. Geophys.* **27**, 3559–3570 (2009)
- Willis, D.M., Lockwood, M., Cowley, S.W.H., Van Eyken, A.P., Bromage, B.J.I., Rishbeth, H., Smith, P.R., Crothers, S.R.: A survey of simultaneous observations of the high latitude ionosphere and interplanetary magnetic field with EISCAT and AMPTE-UKS. *J. Atmos. Terr. Phys.* **48**, 987–1008 (1986)
- Woch, J., Lundin, R.: Magnetosheath plasma precipitation in the polar cusp and its control by the interplanetary magnetic field. *J. Geophys. Res.* **97**, 1421 (1992)
- Zhu, L., Schunk, R.W., Sojka, J.J.: Polar cap arcs: a review. *J. Atmos. Sol. Terr. Phys.* **59**, 1087–1126 (1997)